
Center of Gravity-Guided Focusing Influence Mechanism for Multi-Agent Reinforcement Learning

Yisak Park Sunwoo Lee Seungyul Han*
Graduate School of Artificial Intelligence
UNIST
Ulsan, South Korea 44919
{isaac1018,sunwoolee,syhan}@unist.ac.kr

Abstract

Cooperative multi-agent reinforcement learning (MARL) under sparse rewards presents a fundamental challenge due to limited exploration and insufficient coordinated attention among agents. In this work, we propose the Focusing Influence Mechanism (FIM), a novel framework that enhances cooperation by directing agent influence toward task-critical elements, referred to as Center of Gravity (CoG) state dimensions, inspired by Clausewitz’s military theory. FIM consists of three core components: (1) identifying CoG state dimensions based on their stability under agent behavior, (2) designing counterfactual intrinsic rewards to promote meaningful influence on these dimensions, and (3) encouraging persistent and synchronized focus through eligibility-trace-based credit accumulation. These mechanisms enable agents to induce more targeted and effective state transitions, facilitating robust cooperation even in extremely sparse reward settings. Empirical evaluations across diverse MARL benchmarks demonstrate that the proposed FIM significantly improves cooperative performance compared to baselines.

1 Introduction

Cooperative multi-agent reinforcement learning (MARL) has emerged as a powerful framework for sequential decision-making problems involving multiple agents, with applications in autonomous driving [1], multi-robot coordination [2], and real-time strategy games [3]. These environments typically involve partial observability, making decentralized partially observable Markov decision processes (Dec-POMDPs) [4] a natural modeling choice. To address the challenges arising from limited observability, the centralized training with decentralized execution (CTDE) [5–9] paradigm has been widely adopted. In CTDE, policies are trained using access to the global state and all agents’ observations, but are executed independently using only local observations. Prominent CTDE methods such as VDN [7], QMIX [8], and QPLEX [9] leverage value decomposition to promote coordinated policy learning.

Despite their success, CTDE-based methods often struggle in sparse reward settings where effective exploration is critical [10–12]. To address this, a range of techniques have been explored, including maximizing mutual influence between agents [11], prioritizing under-visited yet important states [13], and diversifying trajectory distributions [14]. While promising, these methods frequently fail to overcome local optima in extremely sparse environments. Our empirical analysis reveals that this is partly due to agents failing to focus on task-critical elements such as objects or opponents, which leads to dispersed behaviors and suboptimal coordination. Without a clear mechanism to guide attention, agents tend to act independently, reducing their collective impact and limiting progress. To overcome this challenge, we take inspiration from Clausewitz’s theory [15] of the Center of

*Correspondence to: Seungyul Han

Gravity (CoG) in military strategy, which emphasizes identifying and concentrating efforts on critical elements central to strategic success. Motivated by this concept, we propose **Focusing Influence Mechanism (FIM)** for MARL, a novel framework that enhances cooperation by directing agent influence toward key task-relevant components.

In our approach, we define Center of Gravity (CoG) state dimensions as those that remain stable across diverse agent behaviors but are critical for task success. FIM integrates three core components to leverage these dimensions. First, a state focusing influence mechanism identifies CoG dimensions based on their low sensitivity to random actions and guides agents to influence them. Second, we introduce counterfactual intrinsic rewards that quantify each agent’s individual contribution to changing these dimensions, aligning local behaviors with global team objectives. Third, an agent focusing influence mechanism employs eligibility traces to encourage synchronized and sustained attention to a shared CoG dimension. These components enable agents to consistently influence meaningful aspects of the environment, resulting in targeted state transitions and improved cooperation even under sparse rewards. Finally, we demonstrate through extensive experiments on several MARL benchmarks that FIM achieves more efficient collaborative performance than existing methods.

2 Related Works

Intrinsic Motivation in Sparse Reward MARL Intrinsic motivation is widely used to promote exploration in sparse-reward environments. Curiosity-driven objectives encourage agents to seek novel or uncertain states [16, 13, 17–20], while trajectory diversity methods aim to expand state-space coverage [21–23]. Committed exploration is induced by conditioning agent behavior on a shared latent variable [24], and spatial formation strategies reduce redundant exploration [25]. Subgoal-based methods decompose tasks into smaller, manageable objectives [26, 27]. Exploration can also be focused in low-dimensional subspaces [12, 28, 29], and expectation alignment allows agents to adapt based on anticipated behaviors of peers [30].

Influence-Driven Coordination Influence-based methods aim to promote coordination by inducing causally significant changes. Social influence frameworks quantify how an agent’s actions affect the behaviors of its teammates [10, 31, 32] and guide communication decisions [33]. Opponent modeling enables agents to influence policy updates of others [34–37]. Influence-aware exploration affect future dynamics [11, 38] or induce novel observations [39]. Influence has been extended to incentivize beneficial behaviors in others [40], discourage undesirable actions [41], or shape the expected returns of other agents [42], as well as to affect external states [43] or latent representations of the environment [44].

Counterfactual Reasoning Based Credit Assignment Counterfactual reasoning facilitates credit assignment by measuring each agent’s contribution to the team’s shared reward. COMA estimates individual action advantages using counterfactual baselines [45–48], while predictive counterfactual models support value decomposition [49, 50]. Shapley value-based methods assign local credit by marginalizing individual contributions to the global reward [51–53]. In offline settings, counterfactual conservatism [54] and sample averaging [55] improve learning stability. Counterfactual reasoning also aids in identifying important agents [56] and salient state [57].

3 Preliminary

Decentralized POMDP and CTDE Setup In MARL, the environment is typically modeled as a Dec-POMDP [4], defined by the tuple $\langle \mathcal{N}, S, A, P, R, O, \mathcal{O}, \gamma \rangle$, where \mathcal{N} is a set of n agents, S is the global state space, $A = A^0 \times \dots \times A^{n-1}$ is the joint action space, and γ is the discount factor. At each timestep t , each agent $i \in \mathcal{N}$ receives a local observation $o_t^i = \mathcal{O}(s_t, i)$ and chooses an action a_t^i from its policy π^i , based on its trajectory $\tau_t^i = (o_0^i, a_0^i, \dots, o_t^i)$. The environment transitions to $s_{t+1} \sim P(\cdot | s_t, \mathbf{a}_t)$ and returns a shared reward $r_t = R(s_t, \mathbf{a}_t)$. The goal is to learn a joint policy $\pi = \prod_{i=1}^n \pi^i$ that maximizes the expected return $\sum_{t=0}^{\infty} r_t$. In this paper, we adopt the CTDE paradigm [8], where agents are trained using global state to optimize a total value function Q^{tot} , while each agent executes actions based solely on local observations during deployment.

Credit Assignment via Counterfactual Reasoning In the CTDE paradigm, credit assignment mechanisms [8, 45, 54, 43] estimate each agent’s contribution to team performance, supporting not only the optimization of a global value function but also promoting effective exploration [14], information sharing [25], and communication [58]. A widely adopted technique is counterfactual reasoning [45, 54, 43], which quantifies causal influence by comparing the actual outcome to a counterfactual one where only an individual agent’s action is replaced. COMA [45], for example, defines credit for agent i as:

$$\text{credit}_t^i = f(s_t, \tau_t, \mathbf{a}_t) - \mathbb{E}_{a_t^i \sim P} [f(s_t, \tau_t, a_t^i, \mathbf{a}_t^{-i})], \quad (1)$$

where $f = Q^{\text{tot}}$ and $P = \pi^i(\cdot|s_t)$. This formulation can generalize to any differentiable objective and has been leveraged not only for advantage estimation but also for shaping exploration and coordination via intrinsic rewards.

Eligibility Trace Eligibility traces are used to implement TD(λ) online by propagating the current TD error to future timesteps for value updates [59]. At each timestep t , the trace $e_t(s)$ is updated as:

$$e_t(s) = \begin{cases} \gamma \lambda e_{t-1}(s) + 1, & \text{if } s = s_t, \\ \gamma \lambda e_{t-1}(s), & \text{otherwise,} \end{cases} \quad (2)$$

where λ is the decay factor. This mechanism accumulates eligibility for recently visited states and decays it over time, focusing value updates on frequently visited states. In this work, we adapt this concept to promote persistent influence on critical states. By extending eligibility traces, we ensure that states with high influence in earlier steps continue to receive attention in subsequent steps, facilitating sustained coordination on task-relevant states.

4 Methodology

4.1 Motivation: The Need for Focusing Influence in Cooperative MARL

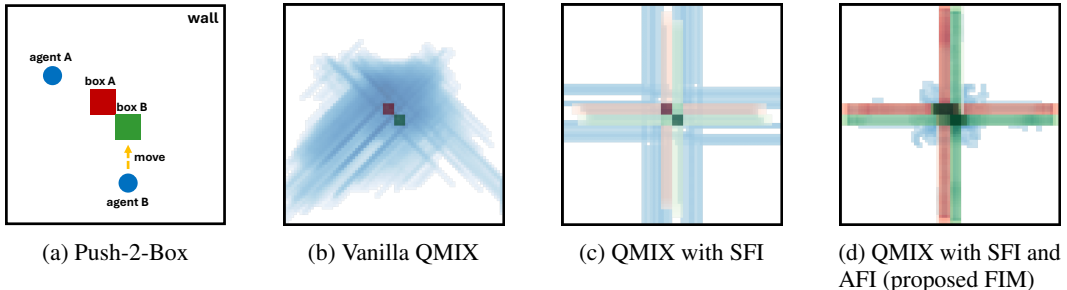


Figure 1: Comparative results in the Push-2-Box environment: (a) shows an enlarged view of the environment, and (b–d) show average visitation counts of two agents (blue) and two boxes (Box A: red, Box B: green) over 3M timesteps across 100 seeds. Darker areas indicate more frequent visits.

In cooperative MARL, agents are often required to solve tasks that cannot be accomplished individually, making effective coordination essential [10–12]. Although CTDE algorithms promote cooperation through centralized training and decentralized execution, they often fail in sparse reward settings where agents struggle to discover meaningful joint behaviors. To illustrate this challenge, we consider the Push-2-Box environment shown in Fig. 1(a), which involves two agents and two boxes. Each box moves one cell when pushed by a single agent and two cells when pushed jointly, requiring synchronized effort to reach the wall within the episode limit. Fig. 1(b) shows the visitation patterns of agents and boxes during training with vanilla QMIX [8], a representative CTDE algorithm. The results reveal scattered exploration and poor coordination, leading to task failure.

This observation underscores the importance of guiding agents to influence specific task-relevant components rather than acting independently. To this end, we propose FIM, a framework that promotes cooperative behavior through two key mechanisms: **state focusing influence (SFI)** and **agent focusing influence (AFI)**. The first mechanism, SFI, identifies Center of Gravity (CoG) state dimensions, which are features that remain stable under random agent behavior but are critical

for task success. Inspired by Clausewitz’s military theory [15], we introduce an entropy-based criterion to systematically select these dimensions. This principled selection represents the first contribution of FIM. We further design a counterfactual intrinsic reward that quantifies each agent’s individual contribution to influencing the CoG dimensions. This reward encourages agents to align their actions with shared objectives and serves as the second contribution of our method. As shown in Fig. 1(c), incorporating SFI into QMIX allows agents to more frequently influence the boxes by focusing on task-relevant components. However, when multiple CoG dimensions are present, agents tend to alternate their focus, leading to unstable coordination and task failure. To address this issue, we introduce AFI, which reinforces synchronized and persistent attention to a shared CoG dimension by using eligibility traces. This mechanism helps stabilize collective behavior and reduces target switching. Fig. 1(d) demonstrates that QMIX with both SFI and AFI, i.e., our proposed FIM framework, enables agents to maintain focus on a single box and successfully complete the task.

While prior work has explored ways to influence states or coordinate agents [14, 60, 27, 43, 25], many rely on heuristics or struggle under truly sparse rewards. In contrast, FIM offers a unified framework that combines principled CoG dimension selection, targeted counterfactual intrinsic rewards, and persistent multi-agent attention via eligibility traces. These components enable more purposeful exploration and robust cooperation, and the next section presents each component of FIM in detail.

4.2 State Focusing Influence via CoG State Dimension Selection

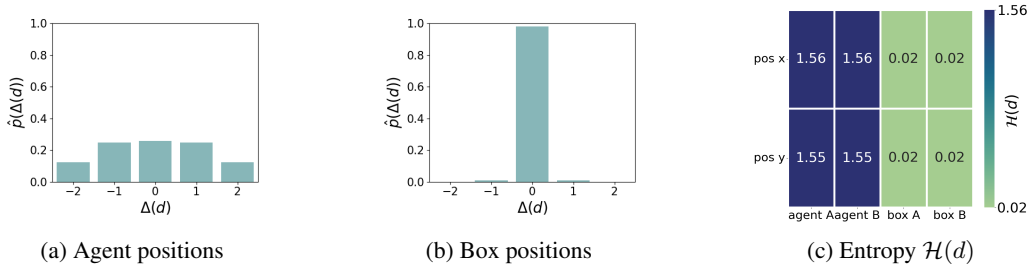


Figure 2: (a–b) Empirical distribution \hat{p} of temporal changes $\Delta(d)$ for agent and box positions, averaged over x, y axes. (c) Entropy $\mathcal{H}(d)$ for each of the 8 state dimensions: (x, y) positions of agent A, agent B, box A, and box B in the Push-2-Box environment. We set the threshold δ to 0.1.

To address the challenge presented in Section 4.1, we introduce a principled approach for identifying Center of Gravity (CoG) state dimensions, which are difficult to influence yet critical for task success. These dimensions remain stable across diverse agent behaviors and cannot be altered without focused effort. Drawing inspiration from military strategy, we introduce a state focusing influence (SFI) mechanism that guides agents to increase their impact on such dimensions. A naive approach might consider the average magnitude of change in each dimension, but this can be misleading: some dimensions fluctuate frequently but trivially, while others exhibit rare yet meaningful changes. To address this, we analyze the diversity of normalized changes under random behavior, enabling us to identify dimensions that are significant for solving task.

To begin, we define the normalized temporal change of dimension $d \in \{0, 1, \dots, D-1\}$, where the global state is denoted as $s_t = (s_t^0, s_t^1, \dots, s_t^{D-1})$, as:

$$\Delta^d(s_t, s_{t+1}) = \frac{s_{t+1}^d - s_t^d}{\mathbb{E}_\rho [|s_{t+1}^d - s_t^d|]}, \quad (3)$$

where ρ is a uniform random policy over the action space, and the denominator normalizes the change using the average magnitude under random trajectories. Next, we compute the Shannon entropy $\mathcal{H}(d)$ of this normalized change to capture its variability:

$$\mathcal{H}(d) = \mathbb{E}_\rho [-\log \hat{p}(\Delta^d(s_t, s_{t+1}) | s_t)], \quad (4)$$

where $\hat{p}(\cdot | s_t)$ denotes the empirical distribution of Δ^d conditioned on s_t , estimated from samples under the random policy ρ . Details of \hat{p} estimation are provided in Appendix B.1. Intuitively, high entropy implies that a dimension responds diversely to random actions (i.e., easily controllable), while low entropy indicates insensitivity to agent behavior.

Based on the computed entropy values, we define the set of CoG state dimensions, which remain relatively unchanged under agent behavior, as:

$$\text{CoG}_\delta = \{d \mid 0 < \mathcal{H}(d) < \delta, d \in \{0, 1, \dots, D-1\}\}, \quad (5)$$

where δ is a selection threshold. Dimensions with zero entropy are excluded as they remain static regardless of agent behavior. To encourage agents to influence these low-entropy CoG dimensions, we design the following counterfactual intrinsic reward:

$$\text{Inf}_t^d(s_t, \mathbf{a}_t, s_{t+1}) = \sum_{i=0}^{n-1} \{|\hat{s}_{t+1}^d(s_t, \mathbf{a}_t) - s_t^d| - \mathbb{E}_{a_t^i \sim \rho^i} [|\hat{s}_{t+1}^d(s_t, a_t^i, \mathbf{a}_t^{-i}) - s_t^d|]\}, d \in \text{CoG}_\delta, \quad (6)$$

where $\hat{s}(\cdot)$ is a learned dynamics model approximating the transition dynamics P , and ρ^i is a random policy for agent i used to simulate counterfactual interventions as introduced in Section 3. Because low-entropy dimensions are typically characterized by limited change under random behavior, directly increasing the magnitude of state transitions in these dimensions naturally leads to increased entropy. Thus, even without explicitly maximizing entropy, our reward effectively encourages agents to explore and influence these stable yet task-relevant components. As a result, agents are guided to discover causally meaningful interactions, which improves exploration efficiency and promotes coordinated behavior in sparse-reward environments.

To visualize the proposed SFI described above, we illustrate the process using the Push-2-Box environment. Fig. 2 shows the empirical distribution \hat{p} of state changes $\Delta(d)$ for (a) agent positions, (b) box positions, and (c) the corresponding entropy of each state dimension. As shown in Fig. 2(c), agent positions, being directly controlled, vary frequently and exhibit high entropy, while box positions change only through coordinated effort, resulting in low entropy. Using a threshold of $\delta = 0.1$, the x and y positions of the box are selected as CoG state dimensions. When the sum of proposed intrinsic reward $\sum_{d \in \text{CoG}_\delta} \text{Inf}_t^d$ is applied, agents focus on these dimensions, leading to more frequent and diverse box movement, as illustrated in Fig. 1(c). This example demonstrates how our method identifies task-relevant but hard-to-change dimensions in practice. In Section 5 and Appendix D.3, we analyze how CoG state dimensions are selected in complex environments and compare our selection method with naive and prior heuristic approaches to show its effectiveness.

4.3 Agent Focusing Influence Based On Eligibility Trace

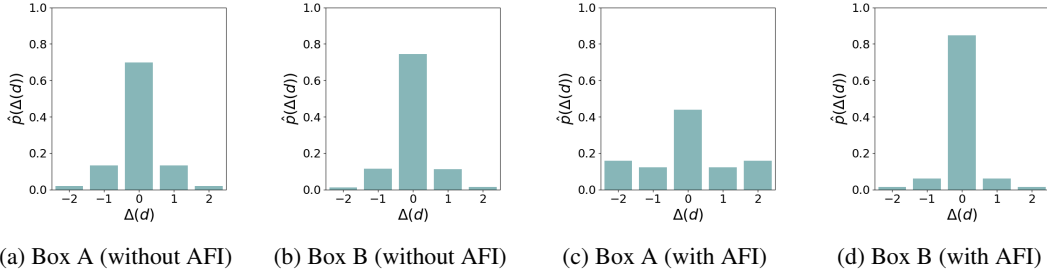


Figure 3: Empirical distribution \hat{p} of temporal changes $\Delta(d)$ for CoG dimensions (box positions): (a–b): Without AFI. (c–d): With AFI, where Box A is the focused target.

While the proposed SFI enables agents to identify critical CoG state dimensions, coordination often becomes unstable when multiple such dimensions are present. Agents may alternate attention across them without maintaining focus, leading to scattered and ineffective behavior. This issue is evident in the Push-2-Box environment introduced in Section 4.1, where agents frequently switch between the two boxes and fail to push either to the wall. Such inconsistency is particularly problematic in tasks that require all agents to jointly influence a single object. To address this, we propose agent focusing influence (AFI), a mechanism that promotes persistent and synchronized attention on a shared CoG dimension through eligibility traces. Specifically, we quantify the current influence on each dimension d as Inf_t^d and update the eligibility trace e_t^d over time as:

$$e_t^d = \lambda \cdot e_{t-1}^d + \eta \cdot \text{Inf}_t^d, d \in \text{CoG}_\delta, \quad (7)$$

where $\lambda \in [0, 1]$ is a decay factor and $\eta > 0$ is a scaling coefficient. The trace e_t accumulates historical influence until time t , increasing as agents repeatedly affect the same dimension.

To guide agents to concentrate on such dimensions, we define an intrinsic reward:

$$r_{\text{int},t} = \sum_{s^d \in \text{CoG}_\delta} w_d \cdot \text{Inf}_t^d \cdot \text{clip}(e_{t-1}^d, 1, c_{\text{max}}), \quad (8)$$

where $w_d = \text{Softmax}(-\mathcal{H}(d))$ prioritizes lower-entropy (harder-to-change) CoG state dimensions, and the clipping operator $\text{clip}(\cdot, 1, c_{\text{max}})$ ensures reward stability (c_{max} set to 10). This design encourages agents to reinforce influence on dimensions they have consistently affected, fostering collective persistence. If a previously focused dimension becomes unreachable (e.g., the target is destroyed or removed), its influence naturally drops, shifting agent attention to the next most relevant CoG dimension. Through this mechanism, agents learn to sequentially commit to one shared target at a time, leading to more robust coordination.

To illustrate the effect of the proposed AFI, Fig. 3 shows how the empirical distribution of temporal changes in CoG state dimensions (i.e., box positions) evolves with and without AFI in the Push-2-Box environment. Without AFI (i.e., $\eta = 0$, $w_d = 1$), applying only SFI, (a) and (b) display greater variation in both boxes compared to vanilla QMIX in Fig. 2(b), indicating increased interaction with CoG dimensions. However, due to lack of focus on a single box, agents split their influence, leading to unstable coordination and task failure. With both SFI and AFI, (c) and (d) show that agents collectively concentrate on Box A, resulting in significantly more variation in its position, while Box B remains mostly unchanged. This focused influence increases entropy for Box A, aligning with successful task completion in Fig. 1(d). This mechanism enables agents to succeed not only in toy tasks but also in more complex multi-agent scenarios. For instance, in combat-style environments, agents can collectively focus on disabling a key opponent, while in soccer-like domains, they may coordinate interference against a specific defender. Even under sparse rewards, this influence-driven reward promotes persistent cooperation and reliable task completion.

By combining the proposed SFI and AFI, we introduce the Focusing Influence Mechanism (FIM) for MARL, which directs each agent’s influence toward CoG state dimensions and encourages collective focus on a single task-relevant target. Agents receive an intrinsic reward $r_{\text{int},t}$ alongside the environment-provided external reward $r_{\text{ext},t}$, forming a total reward $r_t = r_{\text{ext},t} + \alpha r_{\text{int},t}$, where α balances the two terms. We adopt QMIX [8] as the base learner, though our intrinsic reward is model-agnostic and applicable to other MARL algorithms. Further implementation details and the full algorithm of FIM are provided in Appendix B.2.

5 Experiment

In this section, we evaluate the effectiveness of the proposed FIM. We begin with the Push-2-Box task introduced in Section 4.1, comparing various combinations of our proposed components. We then extend the evaluation to more complex MARL benchmarks, the StarCraft Multi-Agent Challenge (SMAC) [61] and Google Research Football (GRF) [62]. In all performance plots, the mean across 5 random seeds is shown as a solid line, and the standard deviation is represented by a shaded area.

5.1 Performance Comparison: Component Evaluation on Push-2-Box

In SFI, agents are guided to influence selected CoG state dimensions using an intrinsic reward $\sum_{d \in \text{CoG}_\delta} \text{Inf}_t^d$ that promotes interaction with low-entropy components. In contrast, AFI applies agent-level focusing across all state dimensions without CoG selection, where the intrinsic reward is given by $\sum_{d=0}^{D-1} \text{Inf}_t^d \cdot \text{clip}(e_{t-1}^d, 1, c_{\text{max}})$. FIM combines both selective targeting and synchronized persistence via the intrinsic reward structure in Eq.(8). We observe that only FIM consistently succeeds in solving the task. Vanilla QMIX alone fails due to ineffective exploration. SFI enhances interaction with critical states, as illustrated in Fig. 1(c), but struggles to maintain consistent focus on a single target, as seen in Fig. 3, which leads to task failure. AFI promotes sustained influence when combined with SFI, yet fails on its own due to the absence of targeted attention. These results emphasize that both principled state selection and agent-level coordination are essential for effective cooperation in sparse-rewarded environments.

We revisit the Push-2-Box task, where two agents must jointly push one of two boxes to a wall, as shown in Fig. 1(a). A box moves by one grid cell if pushed by a single agent and two cells if pushed by both agents. A external reward of +100 is given when either box reaches the wall and -1 is applied if the task fails. The environment is considered successfully solved when agents manage to push a box to the wall within the episode length through synchronized cooperation. More detailed environment settings are provided in Appendix C. Fig. 4 shows the success rate comparison between several baselines: vanilla QMIX trained with only extrinsic rewards, QMIX with SFI, QMIX with AFI, and our full FIM combining both components.

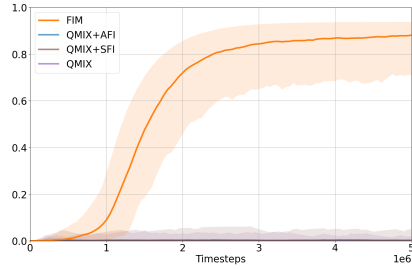


Figure 4: Performance comparison across the proposed focusing components on Push-2-Box environment.

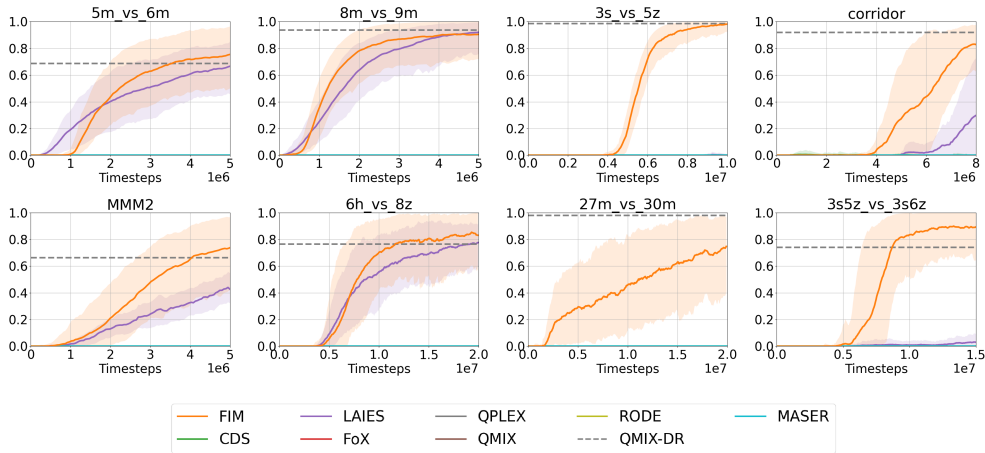


Figure 5: Performance comparison on SMAC environments

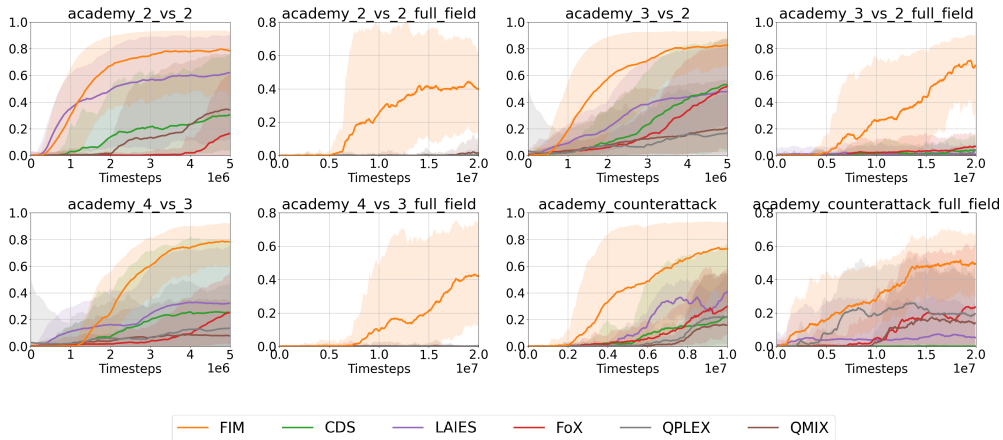


Figure 6: Performance comparison on GRF environments

5.2 Performance Comparison on Complex MARL Benchmarks: SMAC and GRF

Next, we evaluate our method on two complex MARL benchmarks: SMAC and GRF. SMAC is a multi-agent combat environment built on StarCraft II, where agents must coordinate to defeat enemy units. We use a truly sparse reward setting in which agents receive +1 for a win, 0 for a draw, and -1 for a loss. Evaluation is conducted on 8 challenging scenarios: 3 hard maps (5m_vs_6m, 8m_vs_9m, 3s_vs_5z) and 5 super hard maps (corridor, MMM2, 6h_vs_8z, 27m_vs_30m, 3s5z_vs_3s6z), where m, s, z, and h refer to marine, stalker, zealot, and hydralisk units, respectively. GRF is a multi-agent soccer environment where teams compete to score goals under sparse rewards: +100 for a win and -1 for a loss. We evaluate on 8 scenarios, including 4 half-field settings (academy_2_vs_2,

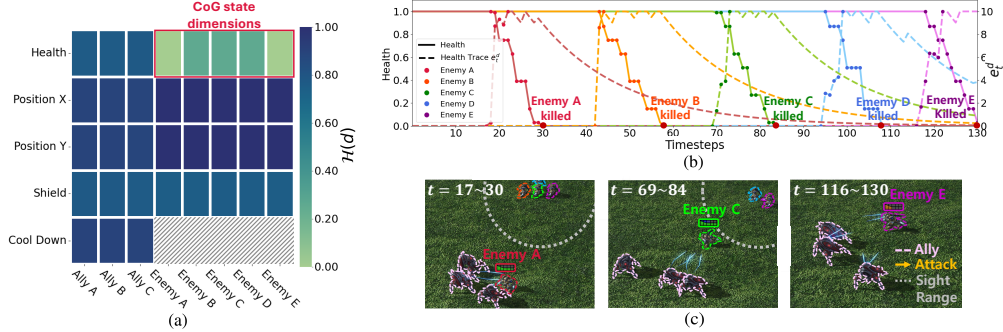


Figure 7: Trajectory analysis in `3s_vs_5z`: (a) Entropy $\mathcal{H}(d)$ with selected CoG state dimensions (b) Changes in enemy health and its trace e_t^d (c) Rendered frames for highlighting agents’ coordination.

`academy_3_vs_2`, `academy_4_vs_3`, `academy_counterattack`) and their corresponding full-field versions, which are more challenging due to the increased field size. Further environment details and visualizations are provided in Appendix C.

For SMAC, we compare FIM against several QMIX-based baselines: **Vanilla QMIX** [8]; **LAIES** [43], which encourages influence over heuristic external state features; **MASER** [27], which identifies subgoals based on Q -values; **CDS** [14], which promotes trajectory diversity for exploration; **FoX** [25], which leverages formation-aware exploration; **RODE** [60], which assigns latent roles to agents; and **QPLEX** [9], which applies monotonic value decomposition with a dueling architecture. For GRF, we compare against Vanilla QMIX, LAIES, CDS, FoX, and QPLEX, omitting baselines without publicly available GRF results. We also include QMIX-DR for SMAC, trained under dense reward settings, to provide an upper-bound reference. Baseline algorithms are evaluated using author-provided implementations, while our method uses the best hyperparameter settings identified through ablation studies. Detailed descriptions of each algorithm, our hyperparameter configurations, and CoG state dimensions for each environment are provided in Appendix D.

Fig. 5 and Fig. 6 present success rate comparisons on the SMAC and GRF benchmarks. In SMAC, QMIX-DR is shown only as a final point to indicate an upper bound under dense rewards. Across both environments, FIM consistently achieves the highest success rates among all baselines. In SMAC, the sparse reward setting poses a significant challenge, as agents must eliminate all enemies without intermediate feedback. While LAIES remains competitive in some scenarios, it struggles on complex maps like `27m_vs_30m` and `corridor`, where it prioritizes influence over external states except ally agents. In contrast, FIM demonstrates robustness by selectively targeting the most critical state dimensions. In GRF, although some baselines perform well on simpler half-field tasks, they largely fail on full-field maps with rare scoring opportunities. FIM, by focusing influence on key components, maintains strong performance across all scenarios. These results highlight that FIM promotes effective cooperation, enabling agents to solve challenging tasks even under highly sparse rewards. For practical comparison, we also evaluate the computational complexity of our method against QMIX in Appendix E. The additional result demonstrates that, with nearly the same training time as QMIX, our method achieves superior performance that is unattainable by the baselines.

5.3 In-depth Analysis and Ablation Studies on SMAC and GRF

To better understand the impact of FIM’s focusing mechanisms, we conduct detailed analyses and ablations in environments where it shows the largest advantage: SMAC’s `3s_vs_5z` and GRF’s `academy_3_vs_2_full_field`. In SMAC `3s_vs_5z`, the state focusing mechanism consistently identifies critical enemy features such as health and shield as CoG state dimensions, as these are crucial for success yet challenging to influence through random behavior. As detailed in Appendix D, similar CoG state dimension patterns are observed in other SMAC environments, while in GRF, the keeper’s position is predominantly selected as a CoG state dimension, as it is challenging for agents to manipulate. These results demonstrate that the proposed method identifies and influences key CoG state dimensions, enhancing performance by focusing on impactful features like health and shield in SMAC and the keeper’s position in GRF.

To further illustrate the effect of the proposed method, Fig. 7(a) presents entropy $\mathcal{H}(d)$ values for each dimension in `3s_vs_5z`, where the health of the five enemy units is selected as CoG dimensions with $\delta = 0.1$. These features change significantly only when agents coordinate attacks. Fig. 7(b) shows

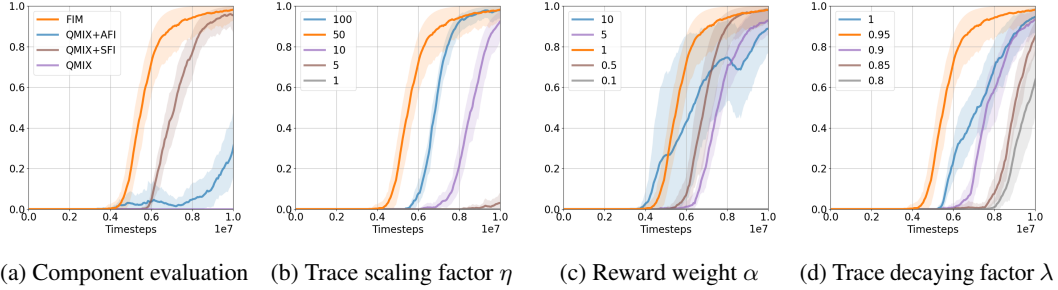


Figure 8: Ablation studies on SMAC 3s_vs_5z

how eligibility traces evolve on enemy health dimensions during an episode, and Fig. 7(c) visualizes key timesteps where enemy units are eliminated. Agents trained with FIM learn to pull enemies into sight and focus fire sequentially. Around $t \approx 20$, they concentrate on the first red enemy, increasing its health trace, and eliminate it by $t \approx 30$. Once removed, its influence drops to zero, and focus shifts to the next enemy (e.g., orange at $t \approx 40$), repeating this process. This strategy resembles human gameplay in StarCraft II. We also provide analysis for GRF in Appendix F, where the results show that agents learn to disrupt the behavior of the keeper, selected as a CoG state dimension, thereby increasing goal-scoring opportunities. These findings demonstrate how FIM promotes structured and effective cooperation even in sparse-reward environments.

Beyond visualization, we conduct ablation studies on 3s_vs_5z to evaluate the contributions of each component and the sensitivity to key hyperparameters. Fig. 8(a) compares performance across the variants considered in Fig. 4: Vanilla QMIX, QMIX with SFI, QMIX with AFI, and the full FIM combining both. Results also show that while SFI and AFI individually improve performance, combining them leads to faster convergence and higher final success rates, confirming the synergy between selective state targeting and synchronized agent coordination. Fig. 8(b)–(d) further examine the effects of the trace scaling factor η , intrinsic reward weight α , and trace decay factor λ . Performance is sensitive to these parameters: too-small values weaken intrinsic rewards and hinder learning, while overly large values lead agents to overfit intrinsic signals and ignore extrinsic rewards. This trade-off is common in intrinsic-motivation-based methods, emphasizing the importance of proper scaling. We set $\eta = 50$, $\alpha = 1$, and $\lambda = 0.95$ as default values based on observed performance. To further evaluate the effectiveness of the proposed method, we provide ablation studies comparing FIM with naive and heuristic state selection approaches, along with results from other environments in Appendix G. FIM consistently outperforms all baselines, further demonstrating the superiority of the CoG state dimension selection method and the overall FIM framework.

6 Limitation

While FIM effectively guides agents to focus on task-critical elements in sparse-reward environments, it assumes the importance of each element remains fixed throughout an episode. In real-world tasks, however, the most relevant target for coordination often changes dynamically. For example, in GRF, advancing the ball is crucial when far from the goal, while disrupting the goalkeeper becomes key near the goal area. Addressing this limitation requires dynamically adapting influence based on the current task context. Additionally, FIM does not consider the timing of influence. In SMAC, concentrating attacks on a single enemy is effective, but if an agent is heavily targeted, prioritizing survival may be necessary. This suggests that both the spatial target and the timing of influence are important. Future work could explore adaptive mechanisms for agents to decide both where and when to apply influence, enabling more context-aware cooperation.

7 Conclusion

In this paper, we address the challenge of efficient cooperation in sparse-reward MARL by proposing FIM, a framework that guides agent influence toward task-critical CoG state dimensions and sustains coordinated focus through eligibility traces. By integrating principled state selection with structured intrinsic rewards based on counterfactual reasoning, FIM enables agents to induce targeted and persistent state transitions. Empirical results across Push-2-Box, SMAC, and GRF demonstrate that FIM significantly improves learning efficiency and coordination, outperforming state-of-the-art baselines. These findings highlight the potential of influence-guided learning to enable robust multi-agent cooperation in complex and sparsely rewarded environments.

References

- [1] Shai Shalev-Shwartz, Shaked Shammah, and Amnon Shashua. Safe, multi-agent, reinforcement learning for autonomous driving. *arXiv preprint arXiv:1610.03295*, 2016.
- [2] Adolfo Perrusquía, Wen Yu, and Xiaou Li. Multi-agent reinforcement learning for redundant robot control in task-space. *International Journal of Machine Learning and Cybernetics*, 12: 231–241, 2021.
- [3] Oriol Vinyals, Igor Babuschkin, Wojciech M Czarnecki, Michaël Mathieu, Andrew Dudzik, Junyoung Chung, David H Choi, Richard Powell, Timo Ewalds, Petko Georgiev, et al. Grandmaster level in starcraft ii using multi-agent reinforcement learning. *nature*, 575(7782):350–354, 2019.
- [4] Frans A Oliehoek, Christopher Amato, et al. *A concise introduction to decentralized POMDPs*, volume 1. Springer, 2016.
- [5] Frans A Oliehoek, Matthijs TJ Spaan, and Nikos Vlassis. Optimal and approximate q-value functions for decentralized pomdps. *Journal of Artificial Intelligence Research*, 32:289–353, 2008.
- [6] Chao Yu, Akash Velu, Eugene Vinitzky, Jiaxuan Gao, Yu Wang, Alexandre Bayen, and YI WU. The surprising effectiveness of ppo in cooperative multi-agent games. In S. Koyejo, S. Mohamed, A. Agarwal, D. Belgrave, K. Cho, and A. Oh, editors, *Advances in Neural Information Processing Systems*, volume 35, pages 24611–24624. Curran Associates, Inc., 2022.
- [7] Peter Sunehag, Guy Lever, Audrunas Gruslys, Wojciech Marian Czarnecki, Vinicius Zambaldi, Max Jaderberg, Marc Lanctot, Nicolas Sonnerat, Joel Z Leibo, Karl Tuyls, et al. Value-decomposition networks for cooperative multi-agent learning based on team reward. In *Proceedings of the 17th International Conference on Autonomous Agents and MultiAgent Systems*, pages 2085–2087, 2018.
- [8] Tabish Rashid, Mikayel Samvelyan, Christian Schroeder, Gregory Farquhar, Jakob Foerster, and Shimon Whiteson. Qmix: Monotonic value function factorisation for deep multi-agent reinforcement learning. In *International Conference on Machine Learning*, pages 4295–4304. PMLR, 2018.
- [9] Jianhao Wang, Zhizhou Ren, Terry Liu, Yang Yu, and Chongjie Zhang. Qplex: Duplex dueling multi-agent q-learning. In *International Conference on Learning Representations*.
- [10] Natasha Jaques, Angeliki Lazaridou, Edward Hughes, Caglar Gulcehre, Pedro Ortega, DJ Strouse, Joel Z Leibo, and Nando De Freitas. Social influence as intrinsic motivation for multi-agent deep reinforcement learning. In *International conference on machine learning*, pages 3040–3049. PMLR, 2019.
- [11] Tonghan Wang, Jianhao Wang, Yi Wu, and Chongjie Zhang. Influence-based multi-agent exploration. In *International Conference on Learning Representations*, 2020.
- [12] Iou-Jen Liu, Unnat Jain, Raymond A Yeh, and Alexander Schwing. Cooperative exploration for multi-agent deep reinforcement learning. In *International conference on machine learning*, pages 6826–6836. PMLR, 2021.
- [13] Lulu Zheng, Jiarui Chen, Jianhao Wang, Jiamin He, Yujing Hu, Yingfeng Chen, Changjie Fan, Yang Gao, and Chongjie Zhang. Episodic multi-agent reinforcement learning with curiosity-driven exploration. *Advances in Neural Information Processing Systems*, 34:3757–3769, 2021.
- [14] Chenghao Li, Tonghan Wang, Chengjie Wu, Qianchuan Zhao, Jun Yang, and Chongjie Zhang. Celebrating diversity in shared multi-agent reinforcement learning. *Advances in Neural Information Processing Systems*, 34:3991–4002, 2021.
- [15] Antulio J Echevarria. Clausewitz’s center of gravity: It’s not what we thought. *Naval War College Review*, 56(1):108–123, 2003.
- [16] Shariq Iqbal and Fei Sha. Coordinated exploration via intrinsic rewards for multi-agent reinforcement learning. *arXiv preprint arXiv:1905.12127*, 2019.

- [17] Jiahui Li, Kun Kuang, Baoxiang Wang, Xingchen Li, Fei Wu, Jun Xiao, and Long Chen. Two heads are better than one: A simple exploration framework for efficient multi-agent reinforcement learning. *Advances in Neural Information Processing Systems*, 36:20038–20053, 2023.
- [18] Shaowei Zhang, Jiahan Cao, Lei Yuan, Yang Yu, and De-Chuan Zhan. Self-motivated multi-agent exploration. In *Proceedings of the 2023 International Conference on Autonomous Agents and Multiagent Systems*, pages 476–484, 2023.
- [19] Kai Yang, Zhirui Fang, Xiu Li, and Jian Tao. Cmbe: Curiosity-driven model-based exploration for multi-agent reinforcement learning in sparse reward settings. In *2024 International Joint Conference on Neural Networks (IJCNN)*, pages 1–8. IEEE, 2024.
- [20] Pei Xu, Junge Zhang, and Kaiqi Huang. Population-based diverse exploration for sparse-reward multi-agent tasks. In *Proceedings of the Thirty-Third International Joint Conference on Artificial Intelligence*, pages 283–291, 2024.
- [21] Yucong Zhang and Chao Yu. Expode: Exploiting policy discrepancy for efficient exploration in multi-agent reinforcement learning. In *Proceedings of the 2023 International Conference on Autonomous Agents and Multiagent Systems*, pages 58–66, 2023.
- [22] Tianxu Li and Kun Zhu. Toward efficient multi-agent exploration with trajectory entropy maximization. In *The Thirteenth International Conference on Learning Representations*, 2025.
- [23] Tianxu Li and Kun Zhu. Learning joint behaviors with large variations. In *Proceedings of the AAAI Conference on Artificial Intelligence*, volume 39, pages 23249–23257, 2025.
- [24] Anuj Mahajan, Tabish Rashid, Mikayel Samvelyan, and Shimon Whiteson. Maven: Multi-agent variational exploration. *Advances in neural information processing systems*, 32, 2019.
- [25] Yonghyeon Jo, Sunwoo Lee, Junghyuk Yeom, and Seungyul Han. Fox: Formation-aware exploration in multi-agent reinforcement learning. In *Proceedings of the AAAI Conference on Artificial Intelligence*, volume 38, pages 12985–12994, 2024.
- [26] Hongyao Tang, Jianye Hao, Tangjie Lv, Yingfeng Chen, Zongzhang Zhang, Hangtian Jia, Chunxu Ren, Yan Zheng, Zhaopeng Meng, Changjie Fan, et al. Hierarchical deep multiagent reinforcement learning with temporal abstraction. *arXiv preprint arXiv:1809.09332*, 2018.
- [27] Jeewon Jeon, Woojun Kim, Whiyoung Jung, and Youngchul Sung. Maser: Multi-agent reinforcement learning with subgoals generated from experience replay buffer. In *International conference on machine learning*, pages 10041–10052. PMLR, 2022.
- [28] Pei Xu, Junge Zhang, Qiyue Yin, Chao Yu, Yaodong Yang, and Kaiqi Huang. Subspace-aware exploration for sparse-reward multi-agent tasks. In *Proceedings of the AAAI Conference on Artificial Intelligence*, volume 37, pages 11717–11725, 2023.
- [29] Xin He, Hongwei Ge, Yaqing Hou, and Jincheng Yu. Saeir: sequentially accumulated entropy intrinsic reward for cooperative multi-agent reinforcement learning with sparse reward. In *Proceedings of the Thirty-Third International Joint Conference on Artificial Intelligence*, pages 4107–4115, 2024.
- [30] Zixian Ma, Rose Wang, Fei-Fei Li, Michael Bernstein, and Ranjay Krishna. Elign: Expectation alignment as a multi-agent intrinsic reward. *Advances in Neural Information Processing Systems*, 35:8304–8317, 2022.
- [31] Pengyi Li, Hongyao Tang, Tianpei Yang, Xiaotian Hao, Tong Sang, Yan Zheng, Jianye Hao, Matthew E Taylor, Wenyuan Tao, and Zhen Wang. Pmic: Improving multi-agent reinforcement learning with progressive mutual information collaboration. In *International Conference on Machine Learning*, pages 12979–12997. PMLR, 2022.
- [32] Yaqing Hou, Jie Kang, Haiyin Piao, Yifeng Zeng, Yew-Soon Ong, Yaochu Jin, and Qiang Zhang. Cooperative multiagent learning and exploration with min–max intrinsic motivation. *IEEE Transactions on Cybernetics*, 2025.

- [33] Ziluo Ding, Tiejun Huang, and Zongqing Lu. Learning individually inferred communication for multi-agent cooperation. *Advances in neural information processing systems*, 33:22069–22079, 2020.
- [34] Jakob Foerster, Richard Y Chen, Maruan Al-Shedivat, Shimon Whiteson, Pieter Abbeel, and Igor Mordatch. Learning with opponent-learning awareness. In *Proceedings of the 17th International Conference on Autonomous Agents and MultiAgent Systems*, pages 122–130, 2018.
- [35] Alistair Letcher, Jakob Foerster, David Balduzzi, Tim Rocktäschel, and Shimon Whiteson. Stable opponent shaping in differentiable games. In *International Conference on Learning Representations*, 2019.
- [36] Annie Xie, Dylan Losey, Ryan Tolsma, Chelsea Finn, and Dorsa Sadigh. Learning latent representations to influence multi-agent interaction. In *Conference on robot learning*, pages 575–588. PMLR, 2021.
- [37] Dong-Ki Kim, Matthew Riemer, Miao Liu, Jakob Foerster, Michael Everett, Chuangchuang Sun, Gerald Tesauro, and Jonathan P How. Influencing long-term behavior in multiagent reinforcement learning. *Advances in Neural Information Processing Systems*, 35:18808–18821, 2022.
- [38] Zeyang Liu, Lipeng Wan, Xinrui Yang, Zhuoran Chen, Xingyu Chen, and Xuguang Lan. Imagine, initialize, and explore: An effective exploration method in multi-agent reinforcement learning. In *Proceedings of the AAAI Conference on Artificial Intelligence*, volume 38, pages 17487–17495, 2024.
- [39] Haobin Jiang, Ziluo Ding, and Zongqing Lu. Settling decentralized multi-agent coordinated exploration by novelty sharing. In *Proceedings of the AAAI Conference on Artificial Intelligence*, volume 38, pages 17444–17452, 2024.
- [40] Jiachen Yang, Ang Li, Mehrdad Farajtabar, Peter Sunehag, Edward Hughes, and Hongyuan Zha. Learning to incentivize other learning agents. *Advances in Neural Information Processing Systems*, 33:15208–15219, 2020.
- [41] Kyrill Schmid, Lenz Belzner, and Claudia Linnhoff-Popien. Learning to penalize other learning agents. In *Artificial Life Conference Proceedings 33*, volume 2021, page 59. MIT Press One Rogers Street, Cambridge, MA 02142-1209, USA journals-info . . . , 2021.
- [42] John L Zhou, Weizhe Hong, and Jonathan Kao. Reciprocal reward influence encourages cooperation from self-interested agents. *Advances in Neural Information Processing Systems*, 37:59491–59512, 2024.
- [43] Boyin Liu, Zhiqiang Pu, Yi Pan, Jianqiang Yi, Yanyan Liang, and Du Zhang. Lazy agents: A new perspective on solving sparse reward problem in multi-agent reinforcement learning. In *International Conference on Machine Learning*, pages 21937–21950. PMLR, 2023.
- [44] Xinran Li, Zifan Liu, Shibo Chen, and Jun Zhang. Individual contributions as intrinsic exploration scaffolds for multi-agent reinforcement learning. In *International Conference on Machine Learning*, pages 28387–28402. PMLR, 2024.
- [45] Jakob Foerster, Gregory Farquhar, Triantafyllos Afouras, Nantas Nardelli, and Shimon Whiteson. Counterfactual multi-agent policy gradients. In *Proceedings of the AAAI conference on artificial intelligence*, volume 32, 2018.
- [46] Andrew Cohen, Ervin Teng, Vincent-Pierre Berges, Ruo-Ping Dong, Hunter Henry, Marwan Mattar, Alexander Zook, and Sujoy Ganguly. On the use and misuse of absorbing states in multi-agent reinforcement learning. *arXiv preprint arXiv:2111.05992*, 2021.
- [47] Jianhao Wang, Zhizhou Ren, Beining Han, Jianing Ye, and Chongjie Zhang. Towards understanding cooperative multi-agent q-learning with value factorization. *Advances in Neural Information Processing Systems*, 34:29142–29155, 2021.

- [48] Heiko Hoppe, Tobias Enders, Quentin Cappart, and Maximilian Schiffer. Global rewards in multi-agent deep reinforcement learning for autonomous mobility on demand systems. In *6th Annual Learning for Dynamics & Control Conference*, pages 260–272. PMLR, 2024.
- [49] Hanhan Zhou, Tian Lan, and Vaneet Aggarwal. Pac: Assisted value factorization with counterfactual predictions in multi-agent reinforcement learning. *Advances in Neural Information Processing Systems*, 35:15757–15769, 2022.
- [50] Jiajun Chai, Yuqian Fu, Dongbin Zhao, and Yuanheng Zhu. Aligning credit for multi-agent cooperation via model-based counterfactual imagination. In *Proceedings of the 23rd International Conference on Autonomous Agents and Multiagent Systems*, pages 281–289, 2024.
- [51] Jianhong Wang, Yuan Zhang, Tae-Kyun Kim, and Yunjie Gu. Shapley q-value: A local reward approach to solve global reward games. In *Proceedings of the AAAI conference on artificial intelligence*, volume 34, pages 7285–7292, 2020.
- [52] Jiahui Li, Kun Kuang, Baoxiang Wang, Furui Liu, Long Chen, Fei Wu, and Jun Xiao. Shapley counterfactual credits for multi-agent reinforcement learning. In *Proceedings of the 27th ACM SIGKDD Conference on Knowledge Discovery & Data Mining*, pages 934–942, 2021.
- [53] Jianhong Wang, Yuan Zhang, Yunjie Gu, and Tae-Kyun Kim. Shaq: Incorporating shapley value theory into multi-agent q-learning. *Advances in Neural Information Processing Systems*, 35:5941–5954, 2022.
- [54] Jianzhun Shao, Yun Qu, Chen Chen, Hongchang Zhang, and Xiangyang Ji. Counterfactual conservative q learning for offline multi-agent reinforcement learning. *Advances in Neural Information Processing Systems*, 36:77290–77312, 2023.
- [55] Jinming Ma and Feng Wu. Learning to coordinate from offline datasets with uncoordinated behavior policies. In *Proceedings of the 2023 International Conference on Autonomous Agents and Multiagent Systems*, pages 1258–1266, 2023.
- [56] Jianming Chen, Yawen Wang, Junjie Wang, Xiaofei Xie, Jun Hu, Qing Wang, and Fanjiang Xu. Understanding individual agent importance in multi-agent system via counterfactual reasoning. In *Proceedings of the AAAI Conference on Artificial Intelligence*, volume 39, pages 15785–15794, 2025.
- [57] Zelei Cheng, Xian Wu, Jiahao Yu, Wenhai Sun, Wenbo Guo, and Xinyu Xing. Statemask: Explaining deep reinforcement learning through state mask. *Advances in Neural Information Processing Systems*, 36:62457–62487, 2023.
- [58] Tonghan Wang, Jianhao Wang, Chongyi Zheng, and Chongjie Zhang. Learning nearly decomposable value functions via communication minimization. In *International Conference on Learning Representations*, 2020.
- [59] Richard S. Sutton and Andrew G. Barto. *Reinforcement Learning: An Introduction*. MIT Press, second edition, 2018. URL <http://incompleteideas.net/book/the-book-2nd.html>.
- [60] Tonghan Wang, Tarun Gupta, Anuj Mahajan, Bei Peng, Shimon Whiteson, and Chongjie Zhang. Rode: Learning roles to decompose multi-agent tasks. In *International Conference on Learning Representations*, 2021.
- [61] Mikayel Samvelyan, Tabish Rashid, Christian Schroeder De Witt, Gregory Farquhar, Nantas Nardelli, Tim GJ Rudner, Chia-Man Hung, Philip HS Torr, Jakob Foerster, and Shimon Whiteson. The starcraft multi-agent challenge. *arXiv preprint arXiv:1902.04043*, 2019.
- [62] Karol Kurach, Anton Raichuk, Piotr Stańczyk, Michał Zajac, Olivier Bachem, Lasse Espeholt, Carlos Riquelme, Damien Vincent, Marcin Michalski, Olivier Bousquet, et al. Google research football: A novel reinforcement learning environment. In *Proceedings of the AAAI conference on artificial intelligence*, volume 34, pages 4501–4510, 2020.
- [63] Jian Hu, Siyang Jiang, Seth Austin Harding, Haibin Wu, and Shih wei Liao. Rethinking the implementation tricks and monotonicity constraint in cooperative multi-agent reinforcement learning. 2021.

A Broader Impact

This work advances cooperative multi-agent systems by introducing a framework that fosters coordinated behavior through influence-based intrinsic motivation. Enhanced cooperation among agents holds strong potential for positive societal impact in domains such as autonomous vehicle coordination, collaborative robotics, disaster response, and environmental monitoring. In these settings, the ability of agents to reason about and influence task-critical aspects collaboratively can lead to more robust, adaptive, and efficient team performance. As a foundational contribution, this research supports the development of AI systems that are better aligned with collective goals, promoting safer and more effective deployment in real-world multi-agent environments.

B Implementation Details

B.1 Empirical Implementation of State Focusing Influence

To estimate $\mathcal{H}(d)$, we approximate the marginal distribution of normalized changes $p(\Delta^d(s_t, s_{t+1}))$, since conditioning on full states $p(\Delta^d(s_t, s_{t+1}) | s_t)$ is computationally prohibitive. We construct the empirical distribution $\hat{p}(\Delta^d(s_t, s_{t+1}))$ by counting occurrences discretized to two decimal places from 100K episodes collected under a random policy. The entropy is then computed as:

$$\mathcal{H}(d) \approx \mathbb{E}_\rho [-\log \hat{p}(\Delta^d(s_t, s_{t+1}))] \quad (9)$$

To ensure comparability across environments, $\mathcal{H}(d)$ values for $d \in \text{CoG}_\delta$ are min-max normalized to the range $[0, 1]$ within each environment.

The counterfactual intrinsic reward in Eq. 6 is computed as the sum of $\text{Inf}_t^{d,i}(\cdot)$ over agents i , where $\text{Inf}_t^{d,i}(\cdot)$ measures the influence of agent i on state dimension s^d at time t :

$$\text{Inf}_t^{d,i}(s_t, \mathbf{a}_t, s_{t+1}) = |\hat{s}_{t+1}^d(s_t, \mathbf{a}_t) - s_t^d| - \mathbb{E}_{a_t^i \sim \rho^i} [|\hat{s}_{t+1}^d(s_t, a_t^i, \mathbf{a}_t^{-i}) - s_t^d|] \quad (10)$$

In practice, the expectation over counterfactual actions $a_t^i \sim \rho^i$ is approximated by uniformly averaging over the set of actions \mathcal{A}_t^i available to agent i at time t , yielding:

$$\text{Inf}_t^{d,i}(s_t, \mathbf{a}_t, s_{t+1}) \approx |\hat{s}_{t+1}^d(s_t, \mathbf{a}_t) - s_t^d| - \frac{1}{|\mathcal{A}_t^i|} \sum_{a_t^i \in \mathcal{A}_t^i} |\hat{s}_{t+1}^d(s_t, a_t^i, \mathbf{a}_t^{-i}) - s_t^d| \quad (11)$$

The transition model \hat{s} used to compute $\text{Inf}_t^{d,i}(\cdot)$ is implemented as a three-layer multilayer perceptron (MLP) and trained by minimizing the following mean squared error loss:

$$\mathcal{L}_{\hat{s}} = \mathbb{E}_{s_t, \mathbf{a}_t, s_{t+1}} [\|\hat{s}(s_t, \mathbf{a}_t) - s_{t+1}\|^2] \quad (12)$$

Since the influence is estimated using a learned model, approximation noise can introduce spurious nonzero signals even when agent i has no actual effect on s^d . To mitigate false positives, we discard any $\text{Inf}_t^{d,i}(\cdot)$ below a threshold κ , and mask out agents that are inactive or dead at time t . The final influence on dimension s^d is computed by summing only the valid contributions:

$$\text{Inf}_t^d(s_t, \mathbf{a}_t, s_{t+1}) = \sum_{i \in \mathcal{N}_t} \mathbf{1}[\text{Inf}_t^{d,i}(s_t, \mathbf{a}_t, s_{t+1}) \geq \kappa] \cdot \text{Inf}_t^{d,i}(s_t, \mathbf{a}_t, s_{t+1}) \quad (13)$$

where \mathcal{N}_t denotes the set of active agents at time t , and $\mathbf{1}[\cdot]$ is the indicator function.

B.2 Complete Implementation and Algorithmic Details of FIM

The FIM framework builds on the centralized training with decentralized execution (CTDE) paradigm, using QMIX to learn a joint action-value function. Each agent maintains an individual Q -function $Q^i(\tau_t^i, a_t^i)$ based on its action-observation history τ_t^i and current action a_t^i . These per-agent utilities are combined via a mixing network to produce a global joint Q -value, $Q_\theta^{\text{tot}}(s_t, \mathbf{a}_t)$, where θ denotes the parameters of the mixing network.

To stabilize learning, FIM employs a target mixing network $Q_{\theta^-}^{\text{tot}}$, which is periodically updated by overwriting its parameters with those of the current mixing network. The temporal difference (TD) loss is computed using a Bellman update that incorporates both extrinsic and intrinsic rewards:

$$\mathcal{L}_{\text{TD}}(\theta) = \mathbb{E}_{s, \mathbf{a}, r, s'} \left[\left(r_{\text{ext}, t} + \alpha r_{\text{int}, t} + \gamma \max_{\mathbf{a}'} Q_{\theta^-}^{\text{tot}}(s_{t+1}, \mathbf{a}') - Q_{\theta}^{\text{tot}}(s_t, \mathbf{a}_t) \right)^2 \right] \quad (14)$$

This loss is minimized using the Adam optimizer to update the parameters θ , while the target network parameters θ^- are synchronized at fixed intervals. The complete training procedure of FIM is summarized in Algorithm 1.

Algorithm 1: FIM framework

Initialize: Q network, dynamics model \hat{s}

- 1 Collect random trajectories under random behavior
 - 2 Approximate $\mathcal{H}(d)$ with the random trajectories based on Eq. (4)
 - 3 Define CoG state dimensions CoG_δ based on Eq. (5)
 - 4 Compute w_d for each $d \in \text{CoG}_\delta$
 - 5 **for** training iteration **do**
 - 6 **for** timestep t **do**
 - 7 Sample transition $(s_t, \mathbf{o}_t, \mathbf{a}_t, s_{t+1}, \mathbf{o}_{t+1})$ using π , where $\mathbf{o}_t = (o_t^0, \dots, o_t^{n-1})$
 - 8 **for** $d \in \text{CoG}_\delta$ **do**
 - 9 Compute collective influence Inf_t^d by Eq. (6)
 - 10 Update eligibility trace e_t^d by Eq. (7)
 - 11 Compute intrinsic reward $r_{\text{int}, t}$ by Eq. (8)
 - 12 Update value function Q^{tot} and dynamics model \hat{s}
-

C Environment Details

Push-2-Box

Push-2-Box is a cooperative multi-agent environment where two agents must jointly push one of two boxes toward a wall to obtain a reward. A box moves one cell if pushed by a single agent and two cells if pushed simultaneously. Thus, synchronized cooperation is essential for completing the task within the episode time limit. The environment terminates either when a box reaches the wall or when the episode length is exceeded.

The **state space** consists of the (x, y) positions of both agents and both boxes, resulting in an 8-dimensional state vector. To isolate coordination from partial observability, each agent receives the full environment state as observation. The **action space** is discrete, consisting of eight movement actions corresponding to up, down, left, right, top-right, right-down, down-left, and left-top directions. The **reward function** is sparse, providing +100 if a box reaches the wall and -1 if no box reaches the wall by the end of the episode.

StarCraft Multi-Agent Challenge (SMAC)

SMAC [61] is a benchmark for evaluating decentralized cooperative multi-agent reinforcement learning. Agents control individual StarCraft II units and must coordinate to defeat enemy forces operated by a scripted AI. During centralized training, a global state is accessible, but during decentralized execution, each agent relies solely on its local observations within a limited sight range. SMAC offers both dense and sparse reward settings, with the sparse reward setting significantly increasing the difficulty by removing intermediate feedback.

The **state space** aggregates absolute features of all units, including positions, health, shields, energies, cooldowns, unit types, and past actions. The **observation space** provides each agent with relative (x, y) positions, health, shield status, and unit types of nearby allies and enemies. The **action space** is discrete, consisting of movement in four directions, attacking visible enemies, stopping, and no-op actions (only allowed for dead units). The **reward function** is summarized in Table 1, and our experiments focus on the sparse reward setting across eight challenging scenarios. Scenario visualizations are provided in Fig. 9, with unit compositions and environment dimensions summarized in Table 2.

Event	Dense reward	Sparse reward
Enemy unit killed	+10 per enemy killed	No reward
Ally unit killed	-10 per ally killed	No reward
Damage dealt to enemy	+ (proportional to damage amount)	No reward
Damage received by ally	- (proportional to damage amount)	No reward
Winning the battle	+200 at episode end	+1 at episode end
Losing the battle	0	-1 at episode end

Table 1: Comparison of dense and sparse reward structures in SMAC

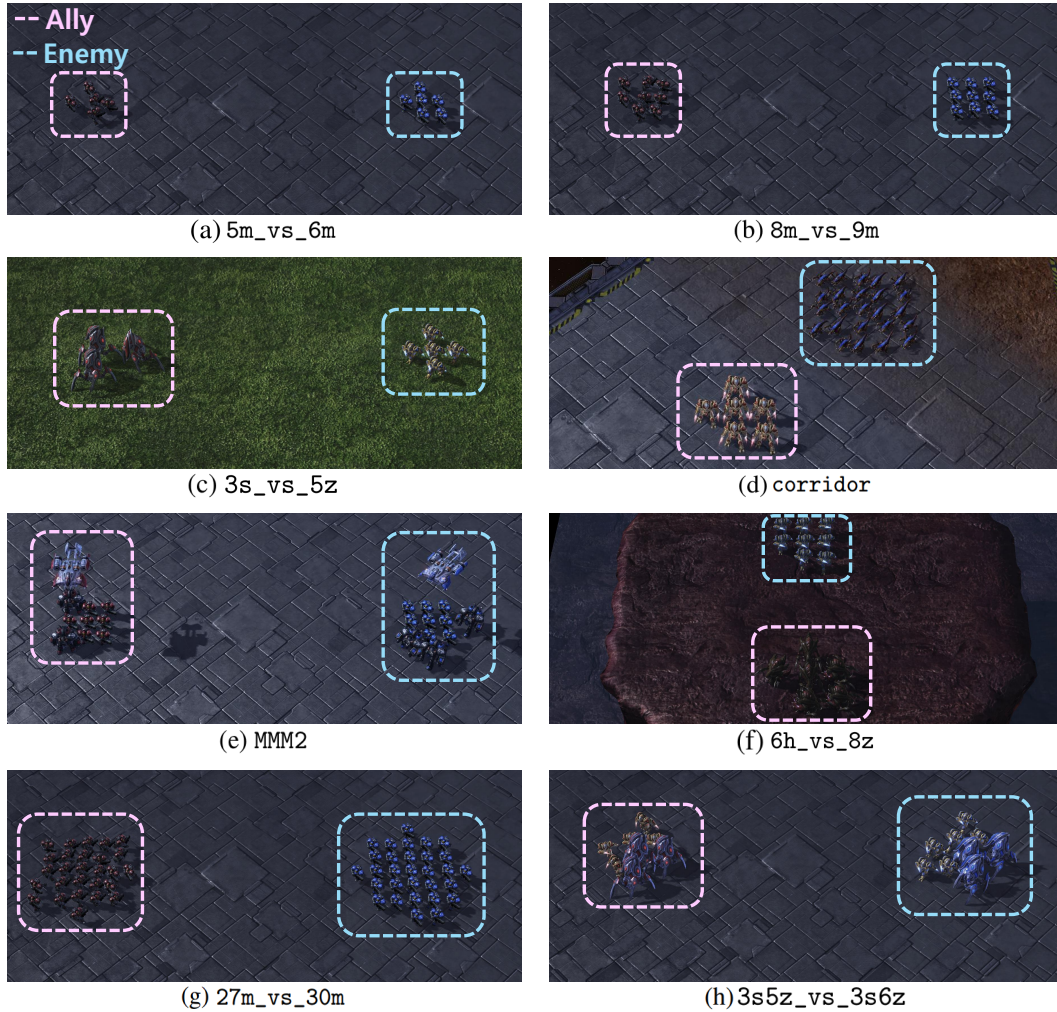


Figure 9: Visualization of initial timestep in SMAC scenarios.

Scenario	Ally	Enemy	State Dim	Obs Dim	Action Dim
5m_vs_6m	5 Marines	6 Marines	98	55	12
8m_vs_9m	8 Marines	9 Marines	179	85	15
3s_vs_5z	3 Stalkers	5 Zealots	68	48	11
corridor	6 Zealots	24 Zerglings	282	156	30
MMM2	1 Medivac, 2 Marauders, 7 Marines	1 Medivac, 3 Marauders, 8 Marines	322	176	18
6h_vs_8z	6 Hydralisks	8 Zealots	140	78	14
27m_vs_30m	27 Marines	30 Marines	1170	285	36
3s5z_vs_3s6z	3 Stalkers, 5 Zealots	3 Stalkers, 6 Zealots	230	136	15

Table 2: SMAC scenario configuration

Google Research Football (GRF)

GRF [62] provides a realistic soccer simulation, incorporating ball dynamics, passing, shooting, tackling, and player movement mechanics. Agents control individual players on a team and must cooperate to score goals against an opponent team controlled by a scripted AI. We adopt a sparse reward setting to evaluate cooperative behavior under severely limited feedback.

The **state space** during centralized training consists of player positions and velocities, as well as ball position and velocity. Each **observation space** for an agent includes local information about the ego player, nearby teammates, opponents, and ball-related features, all expressed relative to the agent’s current frame. The **action space** is discrete, covering movement in eight directions, sliding, passing, shooting, sprinting, and standing still. The **reward function** follows a sparse setting, where agents receive +100 for winning the match and -1 for losing, without intermediate shaping rewards.

For brevity, several GRF scenarios are referred to using abbreviated names. Specifically, `academy_3_vs_2` refers to `academy_3_vs_1_with_keeper`, `academy_2_vs_2` to `academy_run_pass_and_shoot_with_keeper`, `academy_counterattack` to `academy_counterattack_hard`, and `academy_4_vs_3` to `academy_4_vs_2_with_keeper` in the original GRF environment. As shown in Fig. 10, we design full-field variants of these scenarios by repositioning ally and enemy players to opposite half of the court, increasing the difficulty by requiring long-horizon planning and coordinated movement across larger distances. Table 3 provides an overview of the unit configurations and corresponding environment dimensions.

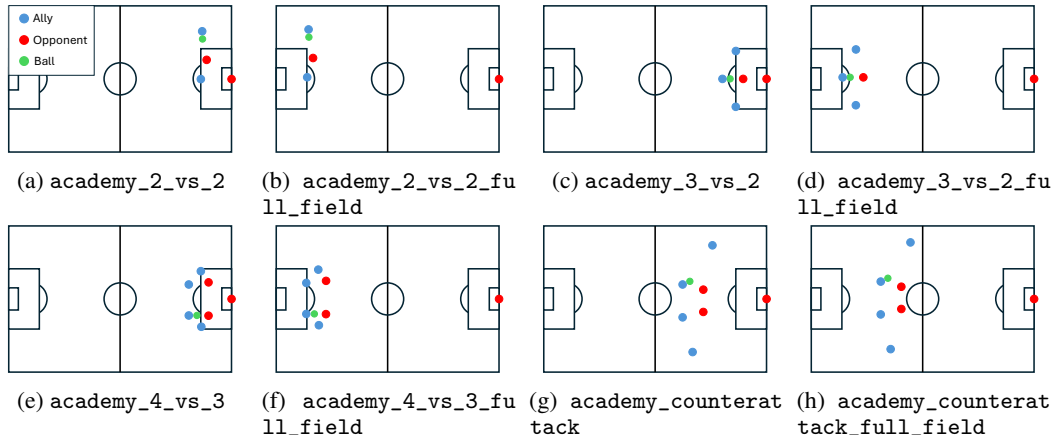


Figure 10: Visualization of initial agent positions in GRF scenarios.

Scenario	Ally	Opponent	State Dim	Obs Dim	Action Dim
academy_2_vs_2	2 center back	1 goalkeeper, 1 center back	22	22	19
academy_2_vs_2 _full_field	2 center back	1 goalkeeper, 1 center back	22	22	19
academy_3_vs_2	3 central midfield	1 goalkeeper, 1 center back	26	26	19
academy_3_vs_2 _full_field	3 central midfield	1 goalkeeper, 1 center back	26	26	19
academy_4_vs_3	4 central midfield	1 goalkeeper, 2 center back	34	34	19
academy_4_vs_3 _full_field	4 central midfield	1 goalkeeper, 2 center back	34	34	19
academy _counterattack	1 central midfield, 1 left midfield, 1 right midfield, 1 central front	1 goalkeeper, 2 center back	34	34	19
academy _counterattack _full_field	1 central midfield, 1 left midfield, 1 right midfield, 1 central front	1 goalkeeper, 2 center back	34	34	19

Table 3: GRF scenario configuration

D Experimental Details

FIM is implemented on top of the open-source framework from [63], which is also used to run QMIX [8] and QPLEX [9]. LAIES [43], RODE [60], MASER [27], CDS [14], and FoX [25] are evaluated using the original code and settings provided by their respective authors. Experiments are conducted on an NVIDIA RTX 3090 GPU with an Intel Xeon Gold 6348 CPU (Ubuntu 20.04). Training completes within two days for Push-2-Box and SMAC, while each GRF scenario requires less than two days to reach 5 million timesteps.

D.1 Detailed Description of Baseline Algorithms

- **QMIX** [8] factorizes the joint action-value function into individual agent utilities, combined via a monotonic mixing network. This ensures that maximizing the global value aligns with individual greedy actions, enabling coordination under decentralized execution. Code: <https://github.com/hijkzzz/pymar12>
- **QPLEX** [9] extends QMIX by using a duplex dueling architecture that decomposes the joint value into individual value and advantage terms. It enforces the Individual-Global-Max (IGM) principle to maintain consistency between joint and individual greedy actions. Code: <https://github.com/hijkzzz/pymar12>
- **LAIES** [43] addresses passive agents by incentivizing influence over external, task-relevant state variables. It uses two intrinsic rewards: one for individual impact via random action substitution and another for joint impact on external states. Code: <https://github.com/liuboyin/LAIES>
- **RODE** [60] improves scalability through hierarchical role-based policies. Agents periodically select discrete roles, constraining their low-level actions to role-specific sets, which enables long-term specialization and coordination. Code: <https://github.com/TonghanWang/RODE>
- **MASER** [27] boosts exploration by generating subgoals from past trajectories. Agents are rewarded based on proximity to assigned subgoals, encouraging revisits to informative states. Code: <https://github.com/Jiwonjeon9603/MASER>

- **CDS** [14] promotes policy diversity under parameter sharing by maximizing mutual information between agent identity and trajectory. This encourages distinguishable behaviors while preserving network efficiency. Code: <https://github.com/lich14/CDS>
- **FoX** [25] fosters structured exploration by maximizing both the entropy of spatial formations and the mutual information between agent behaviors and team structure. This leads to reduction of exploration space and enhanced adaptability in cooperative tasks. Code: <https://github.com/hyeon1996/FoX>

D.2 Hyperparameter Setup of the Proposed FIM

The default hyperparameter settings of FIM, which are generally shared across scenarios, are summarized in Table 4. Scenario-specific tuning of the trace scaling factor η , intrinsic reward weight α , entropy threshold δ , and influence threshold κ is provided in Table 5, while the trace ceiling c_{\max} is fixed at 10, the softmax temperature in $\text{Softmax}(-\mathcal{H}(d))$ is set to 0.1, and the trace decay factor λ is fixed at 0.95 across all scenarios.

Hyperparameters	Value
Optimizer	Adam
ϵ anneal step	50000
Replay buffer size	5000
Target update interval	200
Mini-batch size	32
Mixing network dim	32
Discount factor γ	0.99
Learning rate	0.0005
Dynamics model $\hat{s}(\cdot)$ layer	3
Dynamics model $\hat{s}(\cdot)$ dim	128

Table 4: Common hyperparameter setting of FIM

Scenario	η	α	δ	κ
Push-2-Box	5	0.1	0.1	0
Starcraft Multi-agent Challenge (Sparse)				
5m_vs_6m	50	5	0.05	0.01
8m_vs_9m	50	5	0.05	0.01
3s_vs_5z	50	1	0.1	0.005
corridor	50	5	0.05	0.01
MMM2	50	5	0.15	0.01
6h_vs_8z	50	5	0.1	0.05
27m_vs_30m	50	5	0.05	0.01
3s5z_vs_3s6z	50	5	0.15	0.01
Google Research Football (Sparse)				
academy_2_vs_2	10	1	0.5	0.01
academy_2_vs_2_full_field	10	10	0.5	0.01
academy_3_vs_2	10	10	0.1	0.01
academy_3_vs_2_full_field	10	1	0.1	0.01
academy_4_vs_3	10	10	0.2	0.01
academy_4_vs_3_full_field	10	10	0.2	0.01
academy_counterattack	10	10	0.1	0.01
academy_counterattack_full_field	10	1	0.5	0.001

Table 5: Scenario specific hyperparameter setup of FIM

D.3 Visualization of Entropy $\mathcal{H}(d)$ and CoG State Dimension Selection

Fig. 11 and Fig. 12 visualize $\mathcal{H}(d)$ for SMAC and GRF. To facilitate comparison, $\mathcal{H}(d)$ values are min-max normalized to the range $[0, 1]$ within each environment. In GRF, CoG_δ consistently highlights goalkeeper positions, which are critical for evaluating offensive positioning and shot opportunities, as discussed in Appendix F. In SMAC, it emphasizes enemy health, a key factor for prioritizing targets and coordinating attacks. These results indicate that SFI effectively identifies state dimensions essential for solving the underlying tasks. Although ally-specific features such as unit type, which only change when an agent is eliminated by enemy, are included in the CoG dimensions, FIM emphasizes features that allies can directly influence and thus prioritizes enemy health and shield to increase influence eligibility traces.

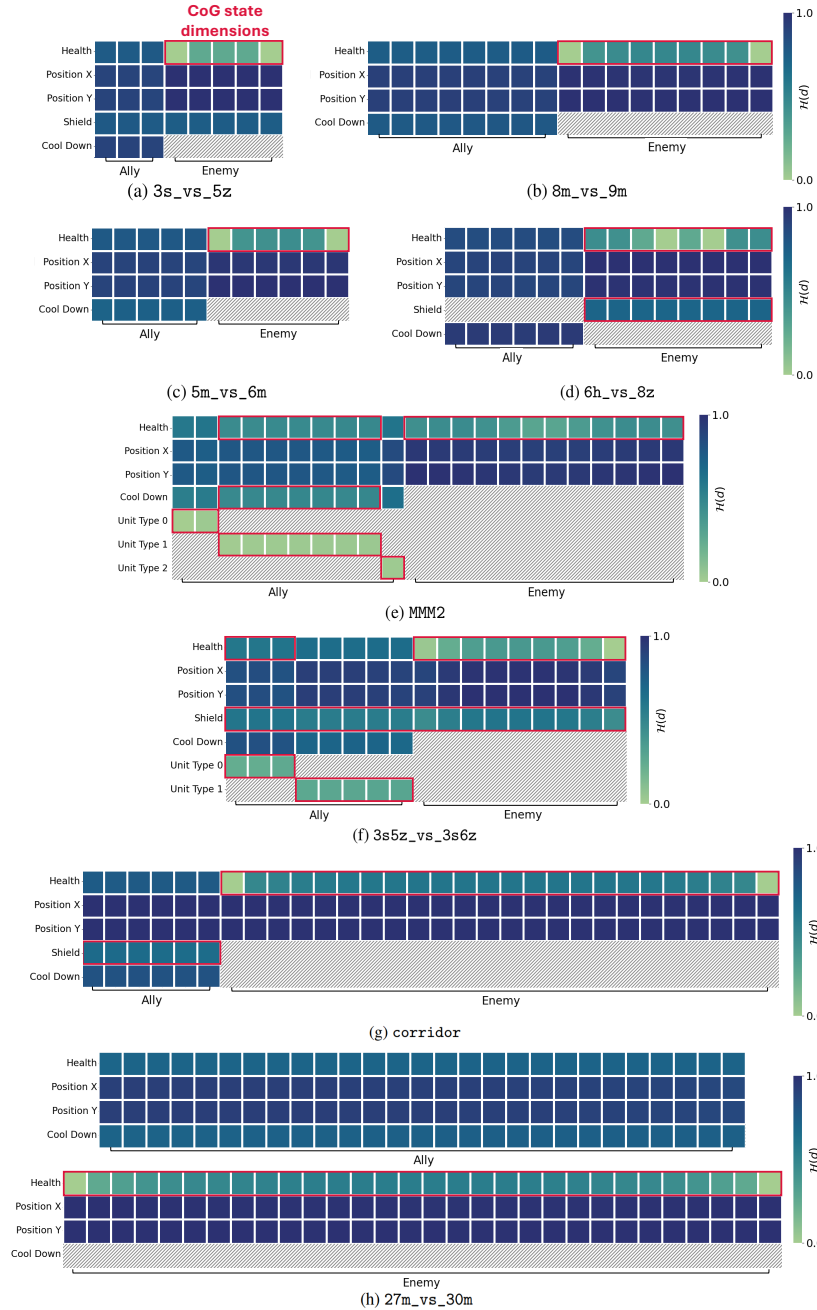


Figure 11: SMAC $\mathcal{H}(d)$ visualization

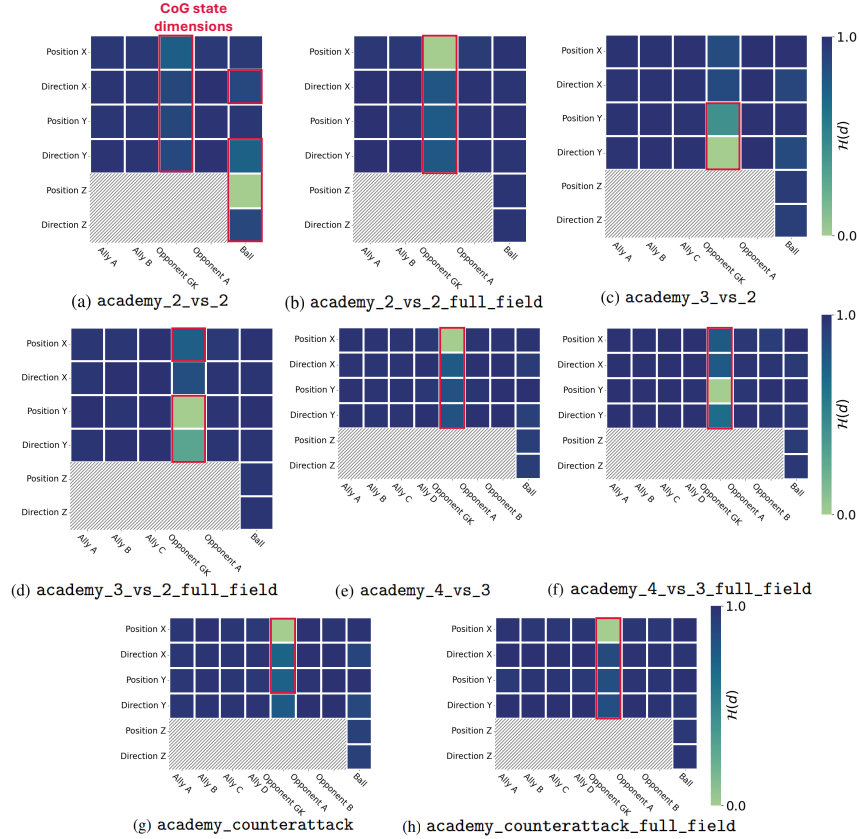


Figure 12: GRF $\mathcal{H}(d)$ visualization

E Comparison of Computational Complexity

FIM computes intrinsic rewards by estimating each agent’s influence through counterfactual marginalization over its action set \mathcal{A} for every dimension in CoG_δ . This results in a space complexity of $O(|\mathcal{N}| \cdot |\mathcal{A}| \cdot |\text{CoG}_\delta|)$ per timestep, while the time complexity remains $O(1)$ due to GPU parallelization. FIM uses a lightweight three-layer multilayer perceptron (MLP) as the forward transition model and does not alter the main Q-network architecture, keeping computational overhead minimal. We compare FIM against QMIX with dense rewards (QMIX-DR), since sparse-reward QMIX often converges to tie-seeking behaviors that avoid conflict [43], resulting in minimal policy updates and unrealistically low computational cost. As shown in Table 6, FIM’s average computation time per 1 million timesteps is comparable to QMIX-DR. In `3s5z_vs_3s6z`, FIM also requires fewer timesteps to reach a 60% success rate, demonstrating strong efficiency. These results emphasize FIM’s ability to enhance agent behavior without compromising computational cost.

Scenario	FIM	QMIX-DR
<code>3s_vs_5z</code>	72.40 min 5.73M	70.65 min 4.21M
<code>3s5z_vs_3s6z</code>	126.43 min 8.26M	123.23 min 13.05M

Table 6: Average computation time (in minutes) per 1 million timesteps (top row) and the number of timesteps (in millions) required to reach a 60% success rate (bottom row).

F Trajectory Analysis in GRF

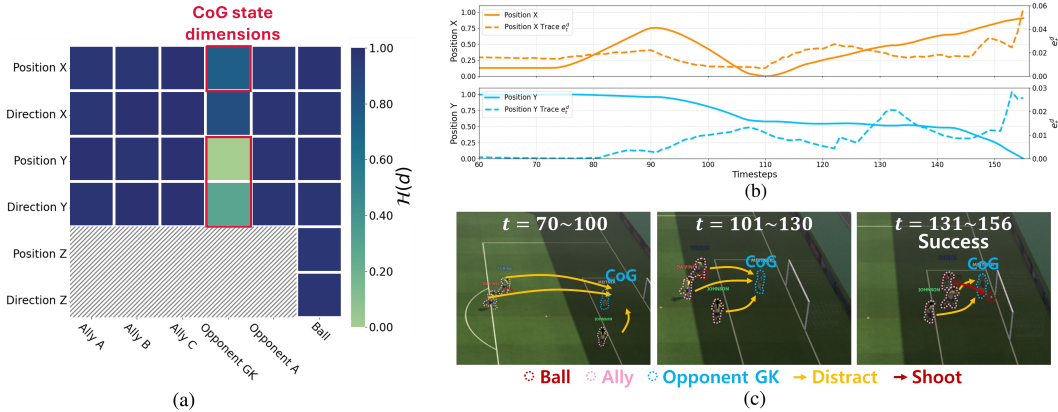


Figure 13: FIM trajectory in GRF academy_3_vs_2_full_field

In GRF, the CoG state dimensions identified by FIM primarily correspond to the position of the opponent goalkeeper, as illustrated in Fig. 13(a). These dimensions exhibit low entropy under random behavior, since the goalkeeper typically remains stationary and only shifts position when a ball-carrying agent approaches the goalpost. This characteristic makes the goalkeeper’s state both stable and strategically significant, as displacing it creates scoring opportunities and thus serves as a valuable proxy objective in sparse reward settings. Accordingly, FIM guides agents to influence the goalkeeper’s position, as it aligns closely with the task objective.

As shown in Fig. 13(b)-(c), this insight is reflected in the agent trajectory. Around $t \approx 70$, agents begin to receive intrinsic rewards by subtly influencing the goalkeeper’s position, even while positioned far from the goal area. By $t \approx 100$, the accumulated eligibility traces further incentivize agents to continue exerting influence over the goalkeeper, enabling a gradual progression toward the goal. Near $t \approx 130$, the goalkeeper briefly moves out of position, and the attacking agent capitalizes on this opportunity to score. Notably, FIM guides agents to approach the goal proactively and maintain persistent influence over the goalkeeper’s positioning, which serves as a task critical factor for successful coordination in this environment, particularly under sparse reward conditions.

G Extended Analysis on Ablation Studies

To further evaluate the robustness of FIM, we conduct experiments on four challenging scenarios: SMAC 3s_vs_5z, SMAC 3s5z_vs_3s6z, GRF academy_3_vs_2, and GRF academy_3_vs_2_full_field. Our analysis focuses on four aspects: (i) alternatives to the SFI state selection mechanism, (ii) the impact of each module in FIM through a component ablation study, (iii) the effect of varying the trace scaling factor η , (iv) the sensitivity to the reward scaling factor α , and (v) the role of the trace decay factor λ in the trace mechanism.

Alternatives to the SFI State Selection Mechanism

We investigate alternative strategies to the SFI state selection mechanism for determining the set of state dimensions to influence: *no-state-selection*, *external state focusing influence* (EFI), and *least-change state focusing influence* (LFI). In all cases, the intrinsic reward is computed as in FIM, with each variant differing only in the selection of the state dimension set \mathcal{D} . The chosen dimensions for each variant are summarized in Table 7. The no-state-selection variant sets \mathcal{D} to include all state dimensions, effectively applying no filtering. EFI manually selects task-relevant external features, following the approach of LAIES [43]: enemy health, shield, and positions in SMAC; and opponent and ball positions and directions in GRF. LFI selects the $n = |\text{CoG}_\delta|$ state dimensions with the smallest average temporal change $|s_{t+1}^d - s_t^d|$ under a random policy. In SMAC, this typically includes enemy health and ally positions, while in GRF, it often selects all direction features due to their relatively small-scale temporal changes.

As shown in Fig. 14, while some SFI variants show comparable performance in (a) and (c), the state dimensions selected by SFI consistently lead to the highest overall performance. When variants include easily influenced features such as ally position, agents tend to exploit these trivial dimensions, leading to reward hacking and suboptimal behavior. These findings underscore the effectiveness of FIM’s entropy-based selection, which identifies stable and causally meaningful CoG dimensions to promote more coordinated and purposeful agent behavior.

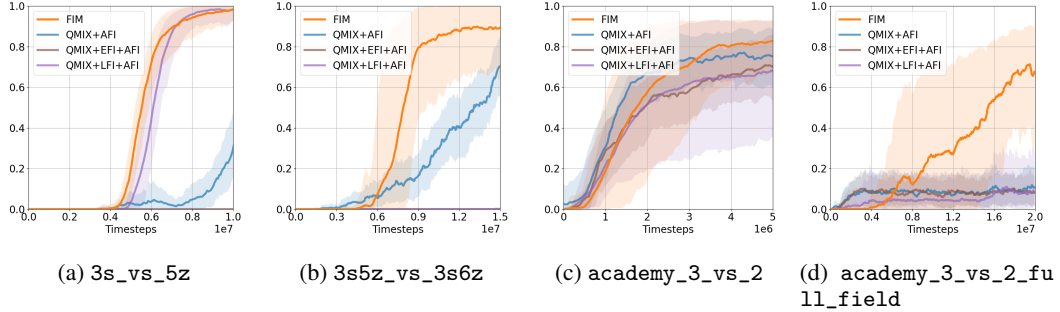


Figure 14: Alternatives to SFI

Scenario	SFI	EFI	LFI
3s_vs_5z	enemy health	enemy health, enemy shield, enemy position	enemy health
3s5z_vs_3s6z	enemy health, enemy shield, ally health, ally shield, ally unit type	enemy health, enemy shield, enemy position	enemy health, enemy position, ally position
academy_3_vs_2	goalkeeper position, goalkeeper direction	opponent position, opponent direction, ball position, ball direction	ally direction
academy_3_vs_2_full_field	goalkeeper position, goalkeeper direction	opponent position, opponent direction, ball position, ball direction	goalkeeper direction, ally direction

Table 7: Selected state dimensions comparison for SFI, EFI and LFI

Component Evaluation

Fig. 15 compares four variants: vanilla QMIX, QMIX with state focusing influence (SFI), QMIX with agent focusing influence (AFI), and the full FIM framework that integrates both components. In SMAC, focused fire emerges as a key cooperative strategy, where agents coordinate to attack a single enemy unit at a time. SFI supports this behavior by directing influence toward task-relevant CoG dimensions, such as enemy health and shield, while AFI encourages agents to maintain consistent attention across time. Although each component improves performance on its own, only their combination in FIM reliably induces and sustains focused fire, resulting in the highest success rates, as shown in Fig. 15(a)-(b). A similar effect is observed in GRF, where SFI identifies the goalkeeper’s position as a key dimension, and AFI ensures that agents continue to influence it over multiple steps in order to exploit brief chance when the goalkeeper is out of position. Together, these components enable coordinated behaviors that consistently outperform all other variants, as shown in Fig. 15(c)-(d).

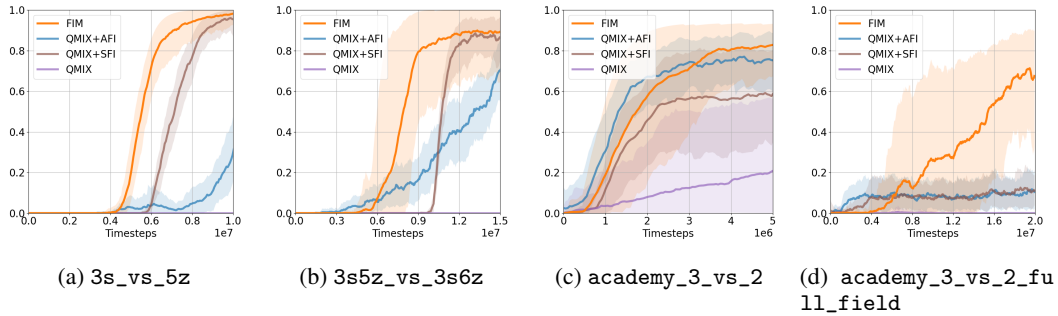


Figure 15: Component evaluation

η Effect Analysis

We investigate how different settings of the trace scaling factor η affect performance by evaluating $\eta \in \{1, 5, 10, 50, 100\}$, as shown in Fig. 16. The results show that the choice of η significantly influences learning outcomes such that extreme values on either end tend to impair performance. When η is too low, a larger amount of influence over a longer period is required to sufficiently increase the eligibility trace, which may cause the system to become insensitive to recent influence and fail to reflect meaningful credit accumulation. On the other hand, if η is too high, the eligibility trace rapidly reaches the ceiling c_{\max} , leading to two undesirable effects. First, it reduces the discriminative power between dimensions, as many attain the same maximum eligibility value. Second, it diminishes the incentive for agents to sustain influence across multiple timesteps, since eligibility values remain near the maximum regardless of temporal decay. Based on these findings, we set $\eta = 50$ for SMAC and $\eta = 10$ for GRF, which yielded the most stable and effective performance across tasks.

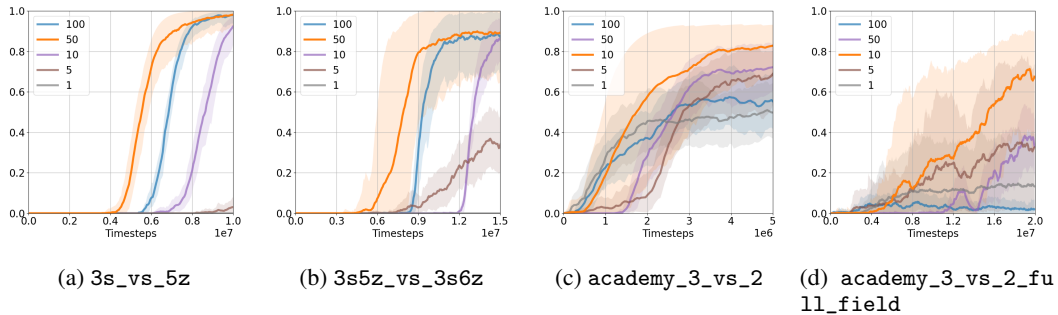


Figure 16: Effect of η

α Effect Analysis

We examine how the reward scaling factor α affects performance by testing values in $\alpha \in \{0.1, 0.5, 1, 5, 10, 50\}$, as shown in Fig. 17. When α is too small, the intrinsic reward signal becomes negligible, preventing agents from effectively learning the influence-guided strategy promoted by FIM. Conversely, setting α too large causes agents to over-prioritize intrinsic rewards, ignoring critical environmental feedback and converging to suboptimal behaviors. To ensure balanced learning, we select α values that are well aligned with the extrinsic reward scale of each scenario. This balance is particularly important in sparse-reward environments, where intrinsic signals must guide exploration without overwhelming the task objective. Our selected α values thus ensure that agents benefit from influence-driven incentives while still grounding their behavior in task success.

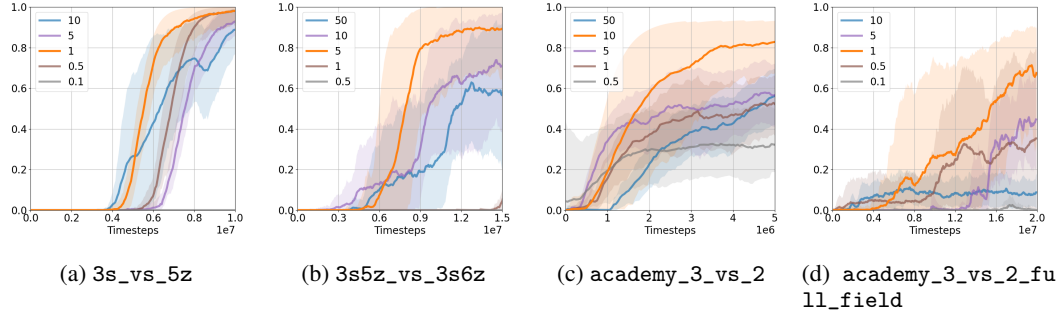


Figure 17: Effect of α

λ Effect Analysis

We examine the effect of the trace decay factor λ by varying it across $\lambda \in \{0.8, 0.85, 0.9, 0.95, 1\}$. The parameter λ determines how long the influence of past actions persists in the eligibility trace. As shown in Fig. 18, when $\lambda = 1$, the trace never decays, causing all past influence, whether recent or outdated, to be treated equally. This undermines the ability to prioritize recent, coordinated influence, weakening short-term focus and resulting in suboptimal performance. Conversely, when λ is too small, eligibility decays too rapidly, limiting the benefit of temporal accumulation and again degrading learning. Through empirical evaluation, we find that $\lambda = 0.95$ consistently yields the best performance and adopt it as the default across all scenarios.

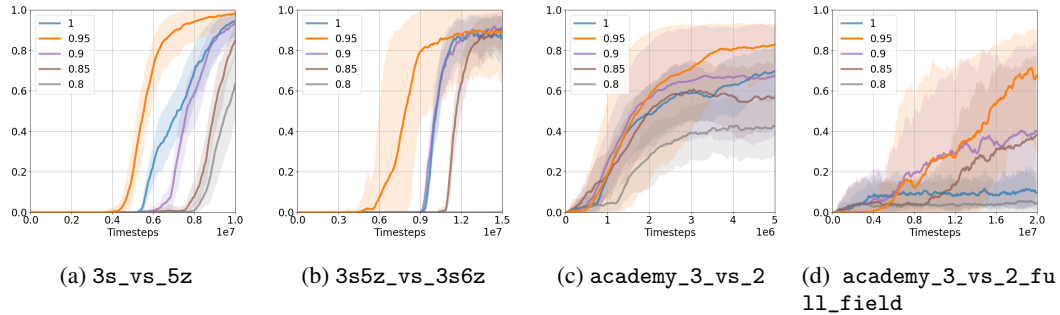


Figure 18: Effect of λ

NeurIPS Paper Checklist

1. Claims

Question: Do the main claims made in the abstract and introduction accurately reflect the paper's contributions and scope?

Answer: [Yes]

Justification: The abstract and introduction (Section 1) clearly and accurately reflect the paper's main contributions and scope.

Guidelines:

- The answer NA means that the abstract and introduction do not include the claims made in the paper.
- The abstract and/or introduction should clearly state the claims made, including the contributions made in the paper and important assumptions and limitations. A No or NA answer to this question will not be perceived well by the reviewers.
- The claims made should match theoretical and experimental results, and reflect how much the results can be expected to generalize to other settings.
- It is fine to include aspirational goals as motivation as long as it is clear that these goals are not attained by the paper.

2. Limitations

Question: Does the paper discuss the limitations of the work performed by the authors?

Answer: [Yes]

Justification: Section 6 highlights that FIM assumes static influence targets and does not account for temporal adaptability.

Guidelines:

- The answer NA means that the paper has no limitation while the answer No means that the paper has limitations, but those are not discussed in the paper.
- The authors are encouraged to create a separate "Limitations" section in their paper.
- The paper should point out any strong assumptions and how robust the results are to violations of these assumptions (e.g., independence assumptions, noiseless settings, model well-specification, asymptotic approximations only holding locally). The authors should reflect on how these assumptions might be violated in practice and what the implications would be.
- The authors should reflect on the scope of the claims made, e.g., if the approach was only tested on a few datasets or with a few runs. In general, empirical results often depend on implicit assumptions, which should be articulated.
- The authors should reflect on the factors that influence the performance of the approach. For example, a facial recognition algorithm may perform poorly when image resolution is low or images are taken in low lighting. Or a speech-to-text system might not be used reliably to provide closed captions for online lectures because it fails to handle technical jargon.
- The authors should discuss the computational efficiency of the proposed algorithms and how they scale with dataset size.
- If applicable, the authors should discuss possible limitations of their approach to address problems of privacy and fairness.
- While the authors might fear that complete honesty about limitations might be used by reviewers as grounds for rejection, a worse outcome might be that reviewers discover limitations that aren't acknowledged in the paper. The authors should use their best judgment and recognize that individual actions in favor of transparency play an important role in developing norms that preserve the integrity of the community. Reviewers will be specifically instructed to not penalize honesty concerning limitations.

3. Theory assumptions and proofs

Question: For each theoretical result, does the paper provide the full set of assumptions and a complete (and correct) proof?

Answer: [NA]

Justification: The paper does not include theoretical results.

Guidelines:

- The answer NA means that the paper does not include theoretical results.
- All the theorems, formulas, and proofs in the paper should be numbered and cross-referenced.
- All assumptions should be clearly stated or referenced in the statement of any theorems.
- The proofs can either appear in the main paper or the supplemental material, but if they appear in the supplemental material, the authors are encouraged to provide a short proof sketch to provide intuition.
- Inversely, any informal proof provided in the core of the paper should be complemented by formal proofs provided in appendix or supplemental material.
- Theorems and Lemmas that the proof relies upon should be properly referenced.

4. Experimental result reproducibility

Question: Does the paper fully disclose all the information needed to reproduce the main experimental results of the paper to the extent that it affects the main claims and/or conclusions of the paper (regardless of whether the code and data are provided or not)?

Answer: [Yes] .

Justification: The paper ensures reproducibility by providing the full code along with detailed hyperparameter settings in Table 4.

Guidelines:

- The answer NA means that the paper does not include experiments.
- If the paper includes experiments, a No answer to this question will not be perceived well by the reviewers: Making the paper reproducible is important, regardless of whether the code and data are provided or not.
- If the contribution is a dataset and/or model, the authors should describe the steps taken to make their results reproducible or verifiable.
- Depending on the contribution, reproducibility can be accomplished in various ways. For example, if the contribution is a novel architecture, describing the architecture fully might suffice, or if the contribution is a specific model and empirical evaluation, it may be necessary to either make it possible for others to replicate the model with the same dataset, or provide access to the model. In general, releasing code and data is often one good way to accomplish this, but reproducibility can also be provided via detailed instructions for how to replicate the results, access to a hosted model (e.g., in the case of a large language model), releasing of a model checkpoint, or other means that are appropriate to the research performed.
- While NeurIPS does not require releasing code, the conference does require all submissions to provide some reasonable avenue for reproducibility, which may depend on the nature of the contribution. For example
 - (a) If the contribution is primarily a new algorithm, the paper should make it clear how to reproduce that algorithm.
 - (b) If the contribution is primarily a new model architecture, the paper should describe the architecture clearly and fully.
 - (c) If the contribution is a new model (e.g., a large language model), then there should either be a way to access this model for reproducing the results or a way to reproduce the model (e.g., with an open-source dataset or instructions for how to construct the dataset).
 - (d) We recognize that reproducibility may be tricky in some cases, in which case authors are welcome to describe the particular way they provide for reproducibility. In the case of closed-source models, it may be that access to the model is limited in some way (e.g., to registered users), but it should be possible for other researchers to have some path to reproducing or verifying the results.

5. Open access to data and code

Question: Does the paper provide open access to the data and code, with sufficient instructions to faithfully reproduce the main experimental results, as described in supplemental material?

Answer: [Yes]

Justification: The code is openly accessible with clear instructions for reproducing the main experimental results.

Guidelines:

- The answer NA means that paper does not include experiments requiring code.
- Please see the NeurIPS code and data submission guidelines (<https://nips.cc/public/guides/CodeSubmissionPolicy>) for more details.
- While we encourage the release of code and data, we understand that this might not be possible, so “No” is an acceptable answer. Papers cannot be rejected simply for not including code, unless this is central to the contribution (e.g., for a new open-source benchmark).
- The instructions should contain the exact command and environment needed to run to reproduce the results. See the NeurIPS code and data submission guidelines (<https://nips.cc/public/guides/CodeSubmissionPolicy>) for more details.
- The authors should provide instructions on data access and preparation, including how to access the raw data, preprocessed data, intermediate data, and generated data, etc.
- The authors should provide scripts to reproduce all experimental results for the new proposed method and baselines. If only a subset of experiments are reproducible, they should state which ones are omitted from the script and why.
- At submission time, to preserve anonymity, the authors should release anonymized versions (if applicable).
- Providing as much information as possible in supplemental material (appended to the paper) is recommended, but including URLs to data and code is permitted.

6. Experimental setting/details

Question: Does the paper specify all the training and test details (e.g., data splits, hyper-parameters, how they were chosen, type of optimizer, etc.) necessary to understand the results?

Answer: [Yes]

Justification: The paper provides all necessary training and testing details, including hyper-parameter settings, ablation studies, and optimizer specifications.

Guidelines:

- The answer NA means that the paper does not include experiments.
- The experimental setting should be presented in the core of the paper to a level of detail that is necessary to appreciate the results and make sense of them.
- The full details can be provided either with the code, in appendix, or as supplemental material.

7. Experiment statistical significance

Question: Does the paper report error bars suitably and correctly defined or other appropriate information about the statistical significance of the experiments?

Answer: [Yes]

Justification: All performance plots report the mean across 5 random seeds with shaded areas denoting standard deviation, as stated in Section 5.

Guidelines:

- The answer NA means that the paper does not include experiments.
- The authors should answer "Yes" if the results are accompanied by error bars, confidence intervals, or statistical significance tests, at least for the experiments that support the main claims of the paper.

- The factors of variability that the error bars are capturing should be clearly stated (for example, train/test split, initialization, random drawing of some parameter, or overall run with given experimental conditions).
- The method for calculating the error bars should be explained (closed form formula, call to a library function, bootstrap, etc.)
- The assumptions made should be given (e.g., Normally distributed errors).
- It should be clear whether the error bar is the standard deviation or the standard error of the mean.
- It is OK to report 1-sigma error bars, but one should state it. The authors should preferably report a 2-sigma error bar than state that they have a 96% CI, if the hypothesis of Normality of errors is not verified.
- For asymmetric distributions, the authors should be careful not to show in tables or figures symmetric error bars that would yield results that are out of range (e.g. negative error rates).
- If error bars are reported in tables or plots, The authors should explain in the text how they were calculated and reference the corresponding figures or tables in the text.

8. Experiments compute resources

Question: For each experiment, does the paper provide sufficient information on the computer resources (type of compute workers, memory, time of execution) needed to reproduce the experiments?

Answer: [Yes]

Justification: Section D specifies the GPU/CPU setup and Section E discusses the time of execution.

Guidelines:

- The answer NA means that the paper does not include experiments.
- The paper should indicate the type of compute workers CPU or GPU, internal cluster, or cloud provider, including relevant memory and storage.
- The paper should provide the amount of compute required for each of the individual experimental runs as well as estimate the total compute.
- The paper should disclose whether the full research project required more compute than the experiments reported in the paper (e.g., preliminary or failed experiments that didn't make it into the paper).

9. Code of ethics

Question: Does the research conducted in the paper conform, in every respect, with the NeurIPS Code of Ethics [https://neurips.cc/public/EthicsGuidelines?](https://neurips.cc/public/EthicsGuidelines)

Answer: [Yes]

Justification: The research uses standard simulation benchmarks without involving human subjects or sensitive data and adheres to NeurIPS ethical guidelines throughout.

Guidelines:

- The answer NA means that the authors have not reviewed the NeurIPS Code of Ethics.
- If the authors answer No, they should explain the special circumstances that require a deviation from the Code of Ethics.
- The authors should make sure to preserve anonymity (e.g., if there is a special consideration due to laws or regulations in their jurisdiction).

10. Broader impacts

Question: Does the paper discuss both potential positive societal impacts and negative societal impacts of the work performed?

Answer: [Yes]

Justification: Societal impacts are discussed in Appendix A and no negative impacts are foreseen.

Guidelines:

- The answer NA means that there is no societal impact of the work performed.
- If the authors answer NA or No, they should explain why their work has no societal impact or why the paper does not address societal impact.
- Examples of negative societal impacts include potential malicious or unintended uses (e.g., disinformation, generating fake profiles, surveillance), fairness considerations (e.g., deployment of technologies that could make decisions that unfairly impact specific groups), privacy considerations, and security considerations.
- The conference expects that many papers will be foundational research and not tied to particular applications, let alone deployments. However, if there is a direct path to any negative applications, the authors should point it out. For example, it is legitimate to point out that an improvement in the quality of generative models could be used to generate deepfakes for disinformation. On the other hand, it is not needed to point out that a generic algorithm for optimizing neural networks could enable people to train models that generate Deepfakes faster.
- The authors should consider possible harms that could arise when the technology is being used as intended and functioning correctly, harms that could arise when the technology is being used as intended but gives incorrect results, and harms following from (intentional or unintentional) misuse of the technology.
- If there are negative societal impacts, the authors could also discuss possible mitigation strategies (e.g., gated release of models, providing defenses in addition to attacks, mechanisms for monitoring misuse, mechanisms to monitor how a system learns from feedback over time, improving the efficiency and accessibility of ML).

11. Safeguards

Question: Does the paper describe safeguards that have been put in place for responsible release of data or models that have a high risk for misuse (e.g., pretrained language models, image generators, or scraped datasets)?

Answer: [NA]

Justification: The paper poses no significant risk of misuse, as it does not release models or datasets with dual-use concerns.

Guidelines:

- The answer NA means that the paper poses no such risks.
- Released models that have a high risk for misuse or dual-use should be released with necessary safeguards to allow for controlled use of the model, for example by requiring that users adhere to usage guidelines or restrictions to access the model or implementing safety filters.
- Datasets that have been scraped from the Internet could pose safety risks. The authors should describe how they avoided releasing unsafe images.
- We recognize that providing effective safeguards is challenging, and many papers do not require this, but we encourage authors to take this into account and make a best faith effort.

12. Licenses for existing assets

Question: Are the creators or original owners of assets (e.g., code, data, models), used in the paper, properly credited and are the license and terms of use explicitly mentioned and properly respected?

Answer: [Yes]

Justification: All used environments and baselines are properly cited in Section 5.

Guidelines:

- The answer NA means that the paper does not use existing assets.
- The authors should cite the original paper that produced the code package or dataset.
- The authors should state which version of the asset is used and, if possible, include a URL.
- The name of the license (e.g., CC-BY 4.0) should be included for each asset.

- For scraped data from a particular source (e.g., website), the copyright and terms of service of that source should be provided.
- If assets are released, the license, copyright information, and terms of use in the package should be provided. For popular datasets, paperswithcode.com/datasets has curated licenses for some datasets. Their licensing guide can help determine the license of a dataset.
- For existing datasets that are re-packaged, both the original license and the license of the derived asset (if it has changed) should be provided.
- If this information is not available online, the authors are encouraged to reach out to the asset's creators.

13. **New assets**

Question: Are new assets introduced in the paper well documented and is the documentation provided alongside the assets?

Answer: [Yes]

Justification: The released code are documented and provided with usage instructions.

Guidelines:

- The answer NA means that the paper does not release new assets.
- Researchers should communicate the details of the dataset/code/model as part of their submissions via structured templates. This includes details about training, license, limitations, etc.
- The paper should discuss whether and how consent was obtained from people whose asset is used.
- At submission time, remember to anonymize your assets (if applicable). You can either create an anonymized URL or include an anonymized zip file.

14. **Crowdsourcing and research with human subjects**

Question: For crowdsourcing experiments and research with human subjects, does the paper include the full text of instructions given to participants and screenshots, if applicable, as well as details about compensation (if any)?

Answer: [NA]

Justification: The research does not involve any human subjects or crowdsourcing.

Guidelines:

- The answer NA means that the paper does not involve crowdsourcing nor research with human subjects.
- Including this information in the supplemental material is fine, but if the main contribution of the paper involves human subjects, then as much detail as possible should be included in the main paper.
- According to the NeurIPS Code of Ethics, workers involved in data collection, curation, or other labor should be paid at least the minimum wage in the country of the data collector.

15. **Institutional review board (IRB) approvals or equivalent for research with human subjects**

Question: Does the paper describe potential risks incurred by study participants, whether such risks were disclosed to the subjects, and whether Institutional Review Board (IRB) approvals (or an equivalent approval/review based on the requirements of your country or institution) were obtained?

Answer: [NA]

Justification: The paper does not involve experiments with human participants requiring IRB or equivalent approval.

Guidelines:

- The answer NA means that the paper does not involve crowdsourcing nor research with human subjects.

- Depending on the country in which research is conducted, IRB approval (or equivalent) may be required for any human subjects research. If you obtained IRB approval, you should clearly state this in the paper.
- We recognize that the procedures for this may vary significantly between institutions and locations, and we expect authors to adhere to the NeurIPS Code of Ethics and the guidelines for their institution.
- For initial submissions, do not include any information that would break anonymity (if applicable), such as the institution conducting the review.

16. Declaration of LLM usage

Question: Does the paper describe the usage of LLMs if it is an important, original, or non-standard component of the core methods in this research? Note that if the LLM is used only for writing, editing, or formatting purposes and does not impact the core methodology, scientific rigorousness, or originality of the research, declaration is not required.

Answer: [NA]

Justification: LLMs were not used in the development of the core methodology of this work.

Guidelines:

- The answer NA means that the core method development in this research does not involve LLMs as any important, original, or non-standard components.
- Please refer to our LLM policy (<https://neurips.cc/Conferences/2025/LLM>) for what should or should not be described.